

The Fundamental Dilemma of Bayesian Active Meta-learning

Sabina J. Sloman^{*1}, Ayush Bharti², and Samuel Kaski^{1,2}

¹Department of Computer Science, University of Manchester, Manchester, UK

²Department of Computer Science, Aalto University, Helsinki, Finland

October 24, 2023

Abstract

Many applications involve estimation of parameters that generalize across multiple diverse, but related, data-scarce task environments. Bayesian active meta-learning, a form of sequential optimal experimental design, provides a framework for solving such problems. The active meta-learner’s goal is to gain transferable knowledge (estimate the transferable parameters) in the presence of idiosyncratic characteristics of the current task (task-specific parameters). We show that in such a setting, greedy pursuit of this goal can actually *hurt* estimation of the transferable parameters (induce so-called negative transfer). The learner faces a dilemma akin to but distinct from the exploration–exploitation dilemma: should they spend their acquisition budget pursuing transferable knowledge, or identifying the current task-specific parameters? We show theoretically that some tasks pose an inevitable and arbitrarily large threat of negative transfer, and that task identification is critical to reducing this threat. Our results generalize to analysis of prior misspecification over nuisance parameters. Finally, we empirically illustrate circumstances that lead to negative transfer.

1 INTRODUCTION

Classical machine learners require access to substantial amounts of data from the environments in which they will be deployed. However, in practice, the daunting task faced by many learners is to bootstrap very little data from several different task environments in order to identify properties that generalize across those tasks. Examples of such a setting include integrative experiments in which data is pooled across many experimental contexts (Almaatouq et al., 2022), learning from the feedback of multiple humans-in-the-loop (Griffith et al., 2013), and learning stable control policies from multiple environments (Mehta et al., 2022). Learning to perform well in multiple tasks that share some underlying structure is the paradigm of *meta-learning* (Kveton et al., 2021; Simchowitz et al., 2021).

We study the setting of active meta-learning, in which we expose an important dilemma. Each task that the active meta-learner encounters has both *transferable* and *task-specific* characteristics. The transferable characteristics correspond to parameter values that are constant across task environments. The task-specific characteristics correspond to task-specific parameters that vary between tasks. The active meta-learner’s primary objective, which we term as *transferable knowledge acquisition*, is to estimate the transferable parameters, which they achieve by taking actions to elicit data in each task that they encounter.

Bayesian active learning, or sequential experimental design (Chaloner and Verdinelli, 1995; Ryan et al., 2016), provides a framework to assess the information the learner can expect to gain from a given action about a quantity of interest. We leverage this framework to measure transferable knowledge acquisition as the information gain about the transferable parameters. We show that greedy pursuit of transferable knowledge measured in this way can *hurt* estimation of the transferable parameters, i.e., result in *negative transfer* (Wang et al. (2019); we define this term within our setting in Section 2).

Figure 1 gives a toy illustration of how negative transfer can occur. In this example, the learner encounters a task characterized by a value of the task-specific parameter (grey horizontal line) that their prior (grey

^{*}Correspondence to sabina.sloman@manchester.ac.uk.

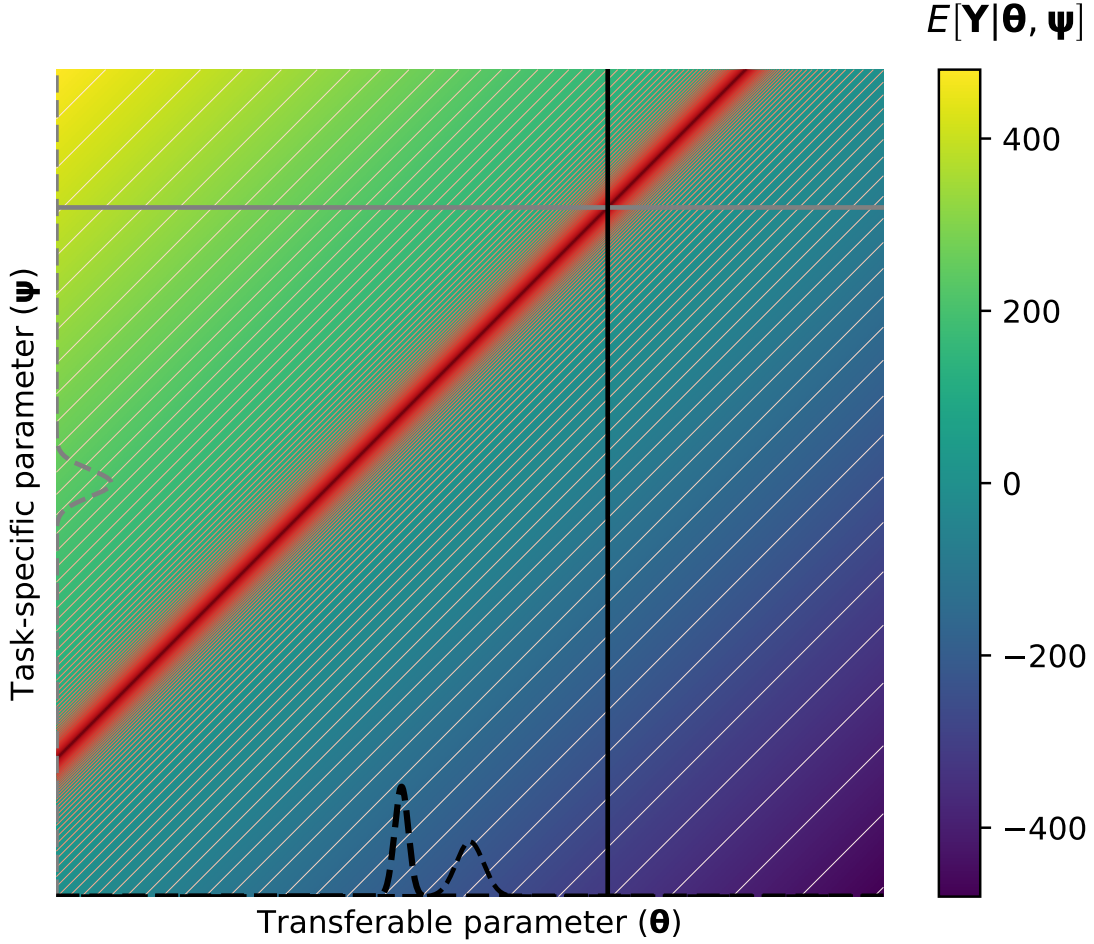


Figure 1: Task-specific dynamics that deviate from the learner’s expectations can result in negative transfer. **Viridis heatmap:** Expected value of \mathbf{y} for different values of the transferable (horizontal axis, denoted θ) and task-specific (vertical axis, denoted ψ) parameters. The expectation of \mathbf{y} is determined as $c(\psi - \theta)$ for a constant c . **Solid lines:** True values of the transferable (black vertical line) and task-specific (grey horizontal line) parameters. **Thin dashed lines:** The learner’s prior over the task-specific (grey line along the vertical axis) and transferable parameters (black line along the horizontal axis). **Red contours:** The true outcome distribution. **Thick dashed line:** The learner’s posterior over the transferable parameter conditioned on an outcome value \mathbf{y} that falls inside the dark red contours (i.e., is likely to be observed).

dashed line) considers unlikely. The result is that their posterior over the transferable parameter (thick black dashed line) moves further from the true value of the transferable parameter (black vertical line) than their prior (thin black dashed line). In other words, the learner was better off *before* learning from data!

In this example, the meta-learner required information of the value of the task-specific parameter in order to achieve their primary objective of transferable knowledge acquisition: conditioning on the true value of the task-specific parameter value would pull their posterior instead towards the true value of the transferable parameter. We term this second, implicit objective *task identification*. Figure 3 shows that, in a similar setting, prioritizing task identification ultimately leads the learner to more accurate inferences.

Of course, the information the learner gathers about task-specific characteristics will, by definition, not generalize to new tasks. This presents the learner with a **meta-learning dilemma**: should an active meta-learner, with a finite acquisition budget, take actions that directly pursue transferable knowledge acquisition, or task identification?

We introduce the paradigm of Bayesian active meta-learning in Section 2. Section 3 provides a set of theoretical results establishing that, in a certain class of particularly threatening settings, negative transfer is both inevitable and can be unboundedly severe (Theorem 3.8) and that task identification is critical to reducing the threat of negative transfer (Theorem 3.9). Based on these results, we construct a principled and novel acquisition function for task identification, and discuss conditions under which acquisition of transferable knowledge is at odds with task identification. Section 4 demonstrates empirically how these results can yield insight and diagnostic tools in two synthetic problem domains.

2 BAYESIAN ACTIVE META-LEARNING

Notation. We denote random variables by bold capital letters (\mathbf{A}), vectors by bold lowercase (\mathbf{a}), and sets by calligraphic capital letters (\mathcal{A}). Let $P_{\mathbf{A}}$ be the distribution of \mathbf{A} and $p(\mathbf{a})$ be the associated density.

Problem setup. The meta-learner encounters tasks sequentially, wherein they can take actions \mathbf{x} from some action set \mathcal{X} . Data acquisition is costly, and so the number of actions they can take in each task is small. Each action \mathbf{x} results in the realization of an outcome variable \mathbf{Y} that can take values $\mathbf{y} \in \mathcal{Y}$. The outcome distribution is determined by \mathbf{x} and the values of some unobservable parameters, partitioned into **transferable parameters** that can take values $\boldsymbol{\theta} \in \mathcal{T}$ and **task-specific parameters** that can take values $\boldsymbol{\psi} \in \mathcal{S}$. The values of the transferable parameters generalize across task environments, while the values of the task-specific parameters differ in each task that the learner encounters. The meta-learner knows this partition, i.e., knows which parameters will transfer, but does not know the true value of $\boldsymbol{\theta}$ or of $\boldsymbol{\psi}$. We use $\boldsymbol{\theta}^*$ and $\boldsymbol{\psi}^*$ to denote, respectively, the true value of the transferable parameters and value of the task-specific parameter that characterize the current task.

The meta-learner’s goal is **transferable knowledge acquisition**, i.e., to identify $\boldsymbol{\theta}^*$. We refer to identification of $\boldsymbol{\psi}^*$ as **task identification**. The meta-learner is interested in task identification only insofar as it facilitates their primary goal of transferable knowledge acquisition. The learner does not have access to the value $\boldsymbol{\theta}^*$ or to $\boldsymbol{\psi}^*$, and so assigns to them a prior distribution $P_{\boldsymbol{\Theta}, \boldsymbol{\Psi}}$. We use P to refer to distributions induced by the learner’s prior, subscripting it to indicate the corresponding random variable. For example, the learner’s expected outcome distribution is $P_{\mathbf{Y}|\mathbf{x}}$, where for any \mathbf{y} , $p(\mathbf{y}|\mathbf{x}) = \mathbb{E}_{\boldsymbol{\theta}, \boldsymbol{\psi} \sim P_{\boldsymbol{\Theta}, \boldsymbol{\Psi}}} [p(\mathbf{y}|\mathbf{x}, \boldsymbol{\theta}, \boldsymbol{\psi})]$, and the learner’s expected outcome distribution delivered under a particular value $\boldsymbol{\theta}$ is $P_{\mathbf{Y}|\mathbf{x}, \boldsymbol{\theta}}$, where for any \mathbf{y} , $p(\mathbf{y}|\mathbf{x}, \boldsymbol{\theta}) = \mathbb{E}_{\boldsymbol{\psi} \sim P_{\boldsymbol{\Psi}|\boldsymbol{\theta}}} [p(\mathbf{y}|\mathbf{x}, \boldsymbol{\theta}, \boldsymbol{\psi})]$.

In each task, the learner encounters a new value $\boldsymbol{\psi}$ drawn from some unknown distribution, which may differ from $P_{\boldsymbol{\Psi}|\boldsymbol{\theta}^*}$. After collecting data (\mathbf{x}, \mathbf{y}) , the learner updates their prior according to Bayes’ rule, i.e., for any $(\boldsymbol{\theta}, \boldsymbol{\psi})$, $p(\boldsymbol{\theta}, \boldsymbol{\psi}|\mathbf{y}, \mathbf{x}) = \frac{p(\mathbf{y}|\mathbf{x}, \boldsymbol{\theta}, \boldsymbol{\psi}) p(\boldsymbol{\theta}, \boldsymbol{\psi})}{p(\mathbf{y}|\mathbf{x})}$.

Sequential optimal experimental design (sOED) (or Bayesian active learning) is an active learning paradigm in which the action \mathbf{x} is selected to maximize the mutual information (I) between the observations it induces and the value of unobservable parameters (see [Ryan et al. \(2016\)](#) or [Rainforth et al. \(2023\)](#) for a review). This quantity is also known as the expected information gain:

Definition 2.1 (Expected information gain (EIG)) (see [Ryan et al. \(2016\)](#), [Rainforth et al. \(2023\)](#), and others)). *The EIG of an action \mathbf{x} is the mutual information between the learner’s expected outcome distribution conditioned on \mathbf{x} and the value $(\boldsymbol{\theta}, \boldsymbol{\psi})$ distributed according to their prior:*

$$\text{EIG}(\mathbf{x}) = I(\boldsymbol{\Theta}, \boldsymbol{\Psi} ; \mathbf{Y}|\mathbf{x}) = \mathbb{E}_{\boldsymbol{\theta}, \boldsymbol{\psi} \sim P_{\boldsymbol{\Theta}, \boldsymbol{\Psi}}} [r(\mathbf{x}, \boldsymbol{\theta}, \boldsymbol{\psi})] \quad (1)$$

where $r(\mathbf{x}, \boldsymbol{\theta}, \boldsymbol{\psi}) := \mathbb{E}_{\mathbf{y} \sim P_{\mathbf{Y}|\mathbf{x}, \boldsymbol{\theta}, \boldsymbol{\psi}}} \left[\log \frac{p(\mathbf{y}|\mathbf{x}, \boldsymbol{\theta}, \boldsymbol{\psi})}{p(\mathbf{y}|\mathbf{x})} \right] = D_{\text{KL}} (P_{\mathbf{Y}|\mathbf{x}, \boldsymbol{\theta}, \boldsymbol{\psi}} \parallel P_{\mathbf{Y}|\mathbf{x}})$ is the learner’s **information gain**.

$D_{\text{KL}} (P_1 \parallel P_2)$ denotes the Kullback-Leibler (KL) divergence from P_1 to P_2 . The active learner endeavors to maximize information about the current task environment, $r(\mathbf{x}, \boldsymbol{\theta}^*, \boldsymbol{\psi}^*)$. However, they do not have access to this due to its dependence on $(\boldsymbol{\theta}^*, \boldsymbol{\psi}^*)$, and so instead maximize an expectation across their prior (Equation (1)). The term “expected information gain” conveys the interpretation of $\text{EIG}(\mathbf{x})$ as the

expectation, across the learner’s prior, of the amount of information the learner will gain about the value of the data-generating parameters.

Because r is a KL divergence measure, it inherits from this measure the property of non-negativity. This means that regardless of the task that the learner encounters, the information gain they experience will be non-negative.

sOED for meta-learning. A naïve active meta-learner greedily maximizes the EIG with respect to the transferable parameters Θ in order to acquire transferable knowledge. We refer to this as the expected transferable information gain:

Definition 2.2 (Expected transferable information gain (ETIG)). *The ETIG of an action \mathbf{x} is the mutual information between the learner’s expected outcome distribution conditioned on \mathbf{x} and the value θ distributed according to their prior:*

$$\text{ETIG}(\mathbf{x}) = I(\Theta ; \mathbf{Y}|\mathbf{x}) = \mathbb{E}_{\theta, \psi \sim P_{\Theta, \Psi}} [r^T(\mathbf{x}, \theta, \psi)] \quad (2)$$

where $r^T(\mathbf{x}, \theta, \psi) := \mathbb{E}_{\mathbf{y} \sim P_{\mathbf{Y}|\mathbf{x}, \theta, \psi}} \left[\log \frac{p(\mathbf{y}|\mathbf{x}, \theta)}{p(\mathbf{y}|\mathbf{x})} \right]$ is the learner’s **transferable information gain**.

The numerator inside the expectation that defines $r^T(\mathbf{x}, \theta, \psi)$ measures the density of $P_{\mathbf{Y}|\mathbf{x}, \theta^*}$ (i.e., the likelihood of $\mathbf{y}|\mathbf{x}$ marginalized across values of ψ). Like EIG, ETIG can be interpreted as the learner’s expectation of the degree to which they will achieve their primary objective; for the meta-learner, this is transferable information gain $r^T(\mathbf{x}, \theta^*, \psi^*)$. We hereafter use $r^{T*}(\mathbf{x}) := r^T(\mathbf{x}, \theta^*, \psi^*)$.

$r^{T*}(\mathbf{x})$ is not a KL divergence measure, and carries no guarantees about whether it is positive or negative, i.e., about whether the meta-learner’s posterior is moving towards or away from θ^* . When the transferable information gain is negative, we say that the meta-learner experiences negative transfer:

Definition 2.3 (Negative transfer). *If $r^{T*}(\mathbf{x}_i) < 0$ for the set of actions \mathbf{x}_i that the learner takes in task i , we say the learner experiences negative transfer in task i .*

Because r^{T*} is not available to the learner, they are unaware of the experience of negative transfer until they transfer their estimate of θ to a new task environment, in which it may poorly predict data from the new task.

3 THEORETICAL RESULTS

In this section, we show that the active meta-learner is faced with a true dilemma: the meta-learner who uses a finite acquisition budget to pursue task identification faces the risk of forgoing transferable knowledge, while the meta-learner who greedily pursues transferable knowledge faces the risk of both arbitrarily high and increasing levels of negative transfer. We first identify the conditions required for negative transfer (Proposition 3.2). This allows us to exhaustively partition the set of tasks the meta-learner could encounter into tasks that are guaranteed to yield positive transfer and “threatening” tasks that are guaranteed to yield negative transfer. Our experimental results (Section 4) show that in some settings, the size of the threatening class can be substantial.

Our main theoretical results are a general set of bounds on r^{T*} (Theorem 3.8), which show that under some conditions the extent of negative transfer cannot be bounded, and Theorem 3.9, which shows that task identification is critical for reducing the threat of negative transfer.

Priors lead to misjudgments. In the example in Figure 1, negative transfer stems from the fact that θ^* induces a completely different distribution of observations under the learner’s prior than under ψ^* . To capture the effect of knowledge of ψ^* on the learner’s expectations, we introduce the concept of misjudgments:

Definition 3.1 (Misjudgment). *We say the learner makes a misjudgment with regards to a function f and distribution P_Ω when for a true value ω^* , $\mathbb{E}_{\omega \sim P_\Omega} [f(\omega)] \neq f(\omega^*)$.*

Proposition 3.2 gives a decomposition of $r^{T^*}(\mathbf{x})$ that reveals that the direction and extent of transferable information gain is affected by two misjudgments. The derivation of Proposition 3.2 is given in Appendix A.3.

Proposition 3.2 (Decomposition of r^{T^*}). *The transferable information gain $r^{T^*}(\mathbf{x})$ can be decomposed as*

$$r^{T^*}(\mathbf{x}) = \underbrace{\text{D}_{\text{KL}}(P_{\mathbf{Y}|\mathbf{x}, \boldsymbol{\theta}^*, \boldsymbol{\psi}^*} \parallel P_{\mathbf{Y}|\mathbf{x}})}_{\text{Predictive misjudgment } (\mathcal{M}_{\text{pred}}(\mathbf{x}))} - \underbrace{\text{D}_{\text{KL}}(P_{\mathbf{Y}|\mathbf{x}, \boldsymbol{\theta}^*, \boldsymbol{\psi}^*} \parallel P_{\mathbf{Y}|\mathbf{x}, \boldsymbol{\theta}^*})}_{\text{Likelihood misjudgment } (\mathcal{M}_L^*(\mathbf{x}))}$$

When the actual outcome distribution, characterized by the density $p(\mathbf{y}|\mathbf{x}, \boldsymbol{\theta}^*, \boldsymbol{\psi}^*)$, differs from the learner's expected outcome distribution, characterized by the density $\mathbb{E}_{\boldsymbol{\theta}, \boldsymbol{\psi} \sim P_{\boldsymbol{\Theta}, \boldsymbol{\Psi}}} [p(\mathbf{y}|\mathbf{x}, \boldsymbol{\theta}, \boldsymbol{\psi})]$, the learner has misjudged the predictive distribution. We use $\mathcal{M}_{\text{pred}}(\mathbf{x})$ to refer to the extent of this **predictive misjudgment**.

When the true likelihood function $p(\mathbf{y}|\mathbf{x}, \boldsymbol{\theta}, \boldsymbol{\psi}^*)$ differs from $p(\mathbf{y}|\mathbf{x}, \boldsymbol{\theta}) = \mathbb{E}_{\boldsymbol{\psi} \sim P_{\boldsymbol{\Psi}|\boldsymbol{\theta}}} [p(\mathbf{y}|\mathbf{x}, \boldsymbol{\theta}, \boldsymbol{\psi})]$, the learner misjudges the likelihood under $\boldsymbol{\theta}$. We use $\mathcal{M}_L(\mathbf{x}, \boldsymbol{\theta}) := \text{D}_{\text{KL}}(P_{\mathbf{Y}|\mathbf{x}, \boldsymbol{\theta}^*, \boldsymbol{\psi}^*} \parallel P_{\mathbf{Y}|\mathbf{x}, \boldsymbol{\theta}})$ to refer to the extent of this **likelihood misjudgment**. $\mathcal{M}_L^*(\mathbf{x})$ refers to the learner's misjudgment of the likelihood under $\boldsymbol{\theta}^*$. Circumstances that pose a threat of negative transfer are those in which $P_{\mathbf{Y}|\mathbf{x}, \boldsymbol{\theta}^*}$ depends on $\boldsymbol{\Psi}$, or in which $\boldsymbol{\theta}$ and $\boldsymbol{\psi}$ interact in determining outcomes. This is what drives the negative transfer in the example in Figure 1: here, $\boldsymbol{\theta}^*$ induces a completely different distribution of observations under the learner's prior than under $\boldsymbol{\psi}^*$.

Before we proceed with our theoretical analysis, we highlight how our results generalize beyond the specific setting studied here. Consider the following generalized version of Definition 3.1:

Definition 3.3 (Generalized misjudgments). *We say the learner makes a generalized misjudgment with regards to a function f and distribution P_Ω when for a true distribution Q_Ω , $\mathbb{E}_{\boldsymbol{\omega} \sim P_\Omega} [f(\boldsymbol{\omega})] \neq \mathbb{E}_{\boldsymbol{\omega} \sim Q_\Omega} [f(\boldsymbol{\omega})]$.*

Definition 3.1 is a special case of Definition 3.3 in which $Q_{\boldsymbol{\Psi}|\boldsymbol{\theta}^*} = \delta(\boldsymbol{\psi}^*)$, where $\delta(\boldsymbol{\psi}^*)$ is the Dirac delta function centered at $\boldsymbol{\psi}^*$. Appendix A states and proves versions of our theoretical results under the generalized definition of misjudgment in Definition 3.3; for the sake of exposition, this main text presents our results under the definition given in Definition 3.1. Our interpretations of these results in the main text pertain to the meta-learner's experience of negative transfer within the context of a given task. The more general interpretation of our results pertains to the correctness of the learner's inferences averaged across multiple values $\boldsymbol{\psi}$, drawn from some distribution which need not match the learner's prior $P_{\boldsymbol{\Psi}|\boldsymbol{\theta}^*}$.

Conditions for negative transfer. Proposition 3.2 states that $r^{T^*}(\mathbf{x})$ is positively related to $\mathcal{M}_{\text{pred}}(\mathbf{x})$ and negatively related to $\mathcal{M}_L^*(\mathbf{x})$. To capture the relative magnitude of $\mathcal{M}_{\text{pred}}(\mathbf{x})$ vs. $\mathcal{M}_L^*(\mathbf{x})$, we characterize the *threat* posed by a particular task.

Definition 3.4 (Threat of negative transfer). *We characterize the following levels of threat of negative transfer:*

1. If $\mathcal{M}_L^*(\mathbf{x}) \leq \mathcal{M}_{\text{pred}}(\mathbf{x})$, we say the task is **non-threatening**, or that we are in the presence of no threat.
2. If $\mathcal{M}_{\text{pred}}(\mathbf{x}) < \mathcal{M}_L^*(\mathbf{x}) \leq \mathbb{E}_{\boldsymbol{\theta} \in P_{\boldsymbol{\Theta}}} [\mathcal{M}_L(\mathbf{x}, \boldsymbol{\theta})]$, we say the task is **mildly threatening**, or that we are in the presence of mild threat.
3. If $\mathbb{E}_{\boldsymbol{\theta} \in P_{\boldsymbol{\Theta}}} [\mathcal{M}_L(\mathbf{x}, \boldsymbol{\theta})] < \mathcal{M}_L^*(\mathbf{x})$, we say the task is **extremely threatening**, or that we are in the presence of extreme threat.

When $\boldsymbol{\psi}^*$ "contaminates" all values $\boldsymbol{\theta}$ equally, $\mathcal{M}_L^*(\mathbf{x}) = \mathbb{E}_{\boldsymbol{\theta} \sim P_{\boldsymbol{\Theta}}} [\mathcal{M}_L(\mathbf{x}, \boldsymbol{\theta})]$ ($\mathcal{M}_{\text{pred}}(\mathbf{x}) \leq \mathbb{E}_{\boldsymbol{\theta} \sim P_{\boldsymbol{\Theta}}} [\mathcal{M}_L(\mathbf{x}, \boldsymbol{\theta})]$) by Lemma A.2, Appendix A.4). When $\mathcal{M}_L^*(\mathbf{x}) < \mathbb{E}_{\boldsymbol{\theta} \sim P_{\boldsymbol{\Theta}}} [\mathcal{M}_L(\mathbf{x}, \boldsymbol{\theta})]$, the learner's misjudgments of the likelihood under $\boldsymbol{\theta}^*$ are on average less egregious than their misjudgment of the likelihood under other possible values of $\boldsymbol{\theta}$. In this sense, $\boldsymbol{\theta}^*$ is not extremely contaminated.

Theorem 3.8 bounds the extent of negative transfer the meta-learner will experience at each threat level. Theorem 3.8 depends on the following definitions:

Definition 3.5 (ϵ -neighborhood of $\boldsymbol{\theta}$ ($N_\epsilon(\boldsymbol{\theta})$)). $N_\epsilon(\boldsymbol{\theta}) := \{\tilde{\boldsymbol{\theta}} \in \mathcal{T} \mid d(\boldsymbol{\theta}, \tilde{\boldsymbol{\theta}}) < \epsilon\}$, where d is a suitable distance measure, is the ϵ -neighborhood of $\boldsymbol{\theta}$.

Definition 3.6 ($\tilde{P}_{\Theta, Y|X}$). $\tilde{P}_{\Theta, Y|X}$ refers to the joint distribution of Θ and $Y|X$ obtained by “subtracting” the contribution of $N_\epsilon(\theta^*)$ from the learner’s prior. \tilde{P}_Θ is the marginal distribution of Θ under $\tilde{P}_{\Theta, Y|X}$, under which

$$\tilde{p}(\theta) := \frac{p(\theta)}{\int_{\mathcal{T} \setminus N_\epsilon(\theta^*)} p(\theta) d\theta} \text{ for any } \theta \in \mathcal{T} \setminus N_\epsilon(\theta^*)$$

and $\tilde{P}_{Y|X}$ is the marginal distribution of $Y|X$ under $\tilde{P}_{\Theta, Y|X}$, under which

$$\tilde{p}(y|X) := \int_{\mathcal{T} \setminus N_\epsilon(\theta^*)} p(y|X, \theta) \tilde{p}(\theta) d\theta \text{ for any } y \in \mathcal{Y}.$$

Theorem 3.8 additionally depends on the following assumption. Our results also apply if the transferable parameter space is discrete, i.e., if P_Θ is a probability mass function, in a way described in Appendix A.4.

Assumption 3.7 (Smoothness in transferable parameter space). *There exists some $\epsilon > 0$ such that*

$$\begin{aligned} & \mathbb{E}_{Y \sim P_{Y|X, \theta^*, \psi^*}} [\log(p(y|X))] \geq \\ & \mathbb{E}_{Y \sim P_{Y|X, \theta^*, \psi^*}} \left[\left(\int_{N_\epsilon(\theta^*)} p(\theta) d\theta \right) \log(p(y|X, \theta^*)) + \left(\int_{\mathcal{T} \setminus N_\epsilon(\theta^*)} p(\theta) d\theta \right) \log(\tilde{p}(y|X)) \right] \end{aligned}$$

Assumption 3.7 allows us to isolate the contribution of $\mathcal{M}_L^*(x)$ to $\mathcal{M}_{\text{pred}}(x)$. It says that, on average across observations $y|X$, there is some ϵ -neighborhood around θ^* inside which the error from approximating the expected likelihood with $p(y|X, \theta^*)$ does not close the Jensen gap between the log marginal likelihood across \mathcal{T} and the expectation of the log marginal likelihood both inside and outside $N_\epsilon(\theta^*)$. If $p(y|X, \theta)$ is smooth near θ^* , one would expect this approximation error to reduce as ϵ approaches 0.

Theorem 3.8 gives bounds on $r^{T^*}(x)$. The proof is given in Appendix A.4. These bounds require access to (θ^*, ψ^*) and so cannot be computed in practice; however, the threat of negative transfer can be assessed on the basis of Monte Carlo samples from the learner’s prior, in ways we demonstrate in Section 4.

Theorem 3.8 (Bounds as a function of the threat of negative transfer). *Given (θ^*, ψ^*) and ϵ that satisfies Assumption 3.7, $r^{T^*}(x)$ is generally upper-bounded as*

$$r^{T^*}(x) \leq \left(\int_{\mathcal{T} \setminus N_\epsilon(\theta^*)} p(\theta) d\theta \right) (\tilde{\mathcal{M}}_{\text{pred}}(x) - \mathcal{M}_L^*(x))$$

where $\tilde{\mathcal{M}}_{\text{pred}}(x) := \text{D}_{\text{KL}}(P_{Y|X, \theta^*, \psi^*} \parallel \tilde{P}_{Y|X})$.

Under the same conditions, $r^{T^*}(x)$ is additionally bounded as follows for each threat level:

1. In the presence of **no threat**, $r^{T^*}(x) \geq 0$.
2. In the presence of **mild threat**, $r^{T^*}(x) < 0$ and $r^{T^*}(x) \geq \mathcal{M}_{\text{pred}}(x) - \mathbb{E}_{\theta \sim P_\Theta} [\mathcal{M}_L(x, \theta)]$.
3. In the presence of **extreme threat**, $r^{T^*}(x) < \mathcal{M}_{\text{pred}}(x) - \mathbb{E}_{\theta \sim P_\Theta} [\mathcal{M}_L(x, \theta)]$. In addition, if $\exists \tilde{\psi}$ such that $\forall \psi < \tilde{\psi}$ or $\forall \psi > \tilde{\psi}$ the following conditions hold:
 - (a) $p(y|X, \theta^*, \psi)$ is well-defined, and
 - (b) if $\psi > \tilde{\psi}$, $\frac{\partial \mathcal{M}_L^*(x)}{\partial \psi} > \frac{\partial \tilde{\mathcal{M}}_{\text{pred}}(x)}{\partial \psi}$ when the derivatives are evaluated at ψ ; else if $\psi < \tilde{\psi}$, $\frac{\partial \mathcal{M}_L^*(x)}{\partial \psi} < \frac{\partial \tilde{\mathcal{M}}_{\text{pred}}(x)}{\partial \psi}$ when the derivatives are evaluated at ψ ,

we can say that $r^{T^*}(x)$ is unbounded below in the sense that $\forall C \in \mathbb{R}$, $\exists \psi$ such that when $\psi^* = \psi$, $r^{T^*}(x) < C$.

If ϵ can be very small without violating Assumption 3.7, $\tilde{\mathcal{M}}_{\text{pred}}(x)$ can be interpreted as the extent of the learner’s predictive misjudgment outside of a very small neighborhood around θ^* .

Theorem 3.8 shows that negative transfer is not only guaranteed when the meta-learner encounters threatening tasks, but that in extremely threatening tasks the extent of negative transfer can be unboundedly large.

Task identification reduces $\mathcal{M}_L^*(\mathbf{x})$. Reducing $\mathcal{M}_L^*(\mathbf{x})$ is a critical part of reducing the threat of negative transfer. Theorem 3.9 shows that the degree to which a task is “unexpected” increases $\mathcal{M}_L^*(\mathbf{x})$:

Theorem 3.9 ($\mathcal{M}_L^*(\mathbf{x})$ decreases with $p(\psi^*|\theta^*)$). *For any $\alpha \in (0, 1]$, conditional on the presence of threat, the lower bound on $\mathcal{M}_L^*(\mathbf{x})$ is lower under the distribution $P_{\Psi|\theta^*}^* := \alpha\delta(\psi^*) + (1 - \alpha)P_{\Psi|\theta^*}$ than under $P_{\Psi|\theta^*}$.*

Importantly, Theorem 3.9 implies that concentration of the learner’s conditional posterior on ψ^* — i.e., task identification — reduces the extent of their likelihood misjudgment.

The information the learner gains about Ψ can be similarly represented in the sOED framework as the expected information gain measure computed with respect to the task-specific parameters Ψ . Theorem 3.9 shows that it is not simply information about Ψ the meta-learner requires, but rather information about Ψ conditioned on θ^* : the magnitude of $\mathcal{M}_L^*(\mathbf{x})$ depends on the measure $p(\psi^*|\theta^*)$. This motivates our definition of expected task-specific information gain, our measure of and proposed acquisition function for achieving task identification:

Definition 3.10 (Expected task-specific information gain (ETSIG)). *The ETSIG of an action \mathbf{x} is the expected mutual information across P_{Θ} between the learner’s expected outcome distribution conditioned on \mathbf{x} and the value $\psi|\theta$ distributed according to their prior:*

$$\begin{aligned} \text{ETSIG}(\mathbf{x}) &= \mathbb{E}_{\theta \sim P_{\Theta}} [I(\Psi|\theta ; \mathbf{Y}|\mathbf{x})] \\ &= \text{EIG}(\mathbf{x}) - \text{ETIG}(\mathbf{x}) \end{aligned} \quad (3)$$

Because the learner does not have access to θ^* , they cannot directly compute $I(\Psi|\theta^* ; \mathbf{Y}|\mathbf{x})$. The ETSIG is thus instead defined as an expectation of $I(\Psi|\theta ; \mathbf{Y}|\mathbf{x})$ with respect to P_{Θ} .

The meta-learning dilemma. The trade-off the learner faces between transferable knowledge acquisition and task identification is transparent in the definition of ETSIG, which depends negatively on the ETIG. Actions that achieve transferable information acquisition may reduce or even eliminate opportunities for task identification. Appendix B gives an example of a simple case in which the action that maximizes ETIG has a corresponding ETSIG of 0.

Notice that if $I(\Psi|\theta^* ; \mathbf{Y}|\mathbf{x}) = 0$, this implies that $\Psi|\theta^*$ and $\mathbf{Y}|\mathbf{x}$ are independent, and so the learner’s posterior over $\Psi|\theta^*$ remains unchanged after viewing data $\mathbf{y}|\mathbf{x}$. When they adopt this posterior as their prior on the next time step, $\mathcal{M}_L^*(\mathbf{x})$ remains unchanged. At the same time, $\mathcal{M}_{\text{pred}}(\mathbf{x})$ decreases as the learner gains information about the joint distribution (Θ, Ψ) . As $\mathcal{M}_{\text{pred}}(\mathbf{x})$ decreases and $\mathcal{M}_L^*(\mathbf{x})$ stays constant, $r^{\text{T}*}(\mathbf{x})$ decreases. In other words, failure to achieve task identification can lead the extent of negative transfer to *increase* as the learner collects more data!

This is the meta-learning dilemma: by directly pursuing transferable knowledge, the active meta-learner risks missing opportunities for task identification and thus the possible exacerbation of negative transfer.

4 EXPERIMENTS

The goal of this section is to illustrate characteristics of meta-learning problems that pose a substantial threat of negative transfer. In two synthetic settings, we demonstrate a substantial threat of negative transfer, and how that threat can be exacerbated by naïve sOED for meta-learning. Further details of the experiments are in Appendix C. All experiments were run using only CPUs.

4.1 Experimental settings

Path analysis in the presence of a latent variable. The first setting corresponds to estimation of a multiple regression model in order to determine the extent to which a particular mechanism of interest is operative. The latent variable takes a value \mathbf{z} , which is unavailable to the experimenter. The values of input variables $\mathbf{x}_{(1)}, \mathbf{x}_{(2)}, \mathbf{x}_{(3)}$ and $\mathbf{x}_{(4)}$ are determined by the value \mathbf{z} . $\mathbf{x}_{(2)}, \mathbf{x}_{(3)}$ and $\mathbf{x}_{(4)}$ are positively correlated with \mathbf{z} ; $\mathbf{x}_{(1)}$, whose effect is the transferable effect of interest to the experimenter, is negatively and inversely correlated with \mathbf{z} . The model is $\mathbf{y} \sim \mathcal{N}(\theta\mathbf{x}_{(1)} + \psi_1\mathbf{x}_{(2)} + \psi_2\mathbf{x}_{(3)} + \psi_3\mathbf{x}_{(4)}, \sigma^2)$.

The interdependency between the effect of θ and the effect of $\{\psi_1, \psi_2, \psi_3\}$ arises because of the effect of \mathbf{z} on the possible values $\{\mathbf{x}_{(1)}, \mathbf{x}_{(2)}, \mathbf{x}_{(3)}, \mathbf{x}_{(4)}\}$. The presence of \mathbf{z} results in a situation qualitatively the same as that shown in Figure 1, in which all available actions result in θ and $\{\psi_1, \psi_2, \psi_3\}$ having opposite effects on \mathbf{y} .

Preference modeling. The second setting corresponds to recovery of a human user’s latent preference function on the basis of their observed choices. Our setting is a version of the preference example from [Foster et al. \(2019\)](#), modified in ways described in Appendix C.2. The model is $\mathbf{y} \sim \text{Bernoulli}\left((1 + e^{\psi\mathbf{x}-\theta})^{-1}\right)$. The transferable parameter θ may correspond to a stable preference that generalizes across users or settings, and ψ may correspond to the accuracy with which a user encodes the choice set in a given setting. Past research has shown that in similar models, interdependency between θ and ψ is induced by the structure of the model ([Krefeld-Schwalb et al., 2022](#)): θ and ψ here have counteracting effects on \mathbf{y} .

4.2 Results

Diagnosing the threat of negative transfer. Figure 2a and Figure 2b divide the parameter space defined by the learner’s prior into regions of no, mild and extreme threat based on the action \mathbf{x}_{ETIG} , i.e., the relative size of $\mathcal{M}_L^*(\mathbf{x}_{\text{ETIG}})$ and $\mathcal{M}_{\text{pred}}(\mathbf{x}_{\text{ETIG}})$ if the corresponding parameter values were the data-generating values, and where \mathbf{x}_{ETIG} is the action that maximizes ETIG. The threatening regions are substantial: in the path analysis example, about 45% of tasks the learner believes they could encounter would induce negative transfer; this is about 25% in the preference example.

Figure 2c and Figure 2d show the corresponding transferable information gain as a function of the value of $p(\psi|\theta^*)$. Notice that, as per Theorem 3.9, the unexpectedness of ψ generally predicts the extent of negative transfer: if $r^T(\mathbf{x}_{\text{ETIG}}, \theta, \psi) < 0$, its magnitude grows with $p(\psi|\theta)$.

Finally, Figure 2e and Figure 2f show the transferable information gain yielded by \mathbf{x}_{ETIG} ($r^{T*}(\mathbf{x}_{\text{ETIG}})$) vs. the maximum transferable information gain achievable ($\max_{\mathbf{x}} r^{T*}(\mathbf{x})$). In many cases (orange regions) pursuing naïve sOED results in negative transfer, which the learner could avoid by taking another action.

Importantly, creation of Figure 2a–Figure 2f requires no knowledge of (θ^*, ψ^*) . These results are instead pre-emptive diagnostics that can be used in practice to assess the risk of negative transfer.

Simulated experiments. Figure 3 shows simulated experiments run in the presence of no, mild and extreme threat. Figure 3a and Figure 3b show experiments under values (θ^*, ψ^*) for which $\mathcal{M}_L^*(\mathbf{x}_{\text{ETIG}}) < \mathcal{M}_{\text{pred}}(\mathbf{x}_{\text{ETIG}})$ at the beginning of the experiment, i.e., before the learner has updated their prior on the basis of data. Figure 3c–Figure 3d and Figure 3e–Figure 3f show experiments for which the conditions of mild and extreme threat, respectively, hold in the same way (i.e., at the beginning of the experiments). Experiments are run under two acquisition functions: naïve sOED selects the action that maximizes ETIG on every time step; the “oracle” method can compute r^{T*} , and maximizes ETIG if there is no threat of negative transfer and ETSIG otherwise.

Figure 3 shows that negative transfer is experienced in the presence of threat, and is more extreme in the presence of extreme threat (Figure 3c–Figure 3f; in the path analysis setting, the gap $\mathbb{E}_{\theta \sim P_{\Theta}} [\mathcal{M}_L(\mathbf{x}, \theta)] - \mathcal{M}_{\text{pred}}(\mathbf{x})$ is so small that tasks in this region have essentially matching lower and upper bounds at 0). In these cases, task identification generally helps, especially in the presence of extreme threat, where the oracle method consistently leads to less extreme negative transfer than naïve sOED.

5 RELATED WORK

Online learning with distribution shift. Meta-learning is related to other paradigms such as active transfer learning, or active learning in the presence of covariate shift, in which the learner aims to predict in a target environment but can learn only from data in a different source environment ([Sugiyama et al., 2008](#); [Peng et al., 2020](#); [Zhao et al., 2021](#)), and continual (or lifelong) learning, in which the learner encounters a continual stream of data and aims to both learn and retain insights from past data ([Javed and White, 2019](#)).

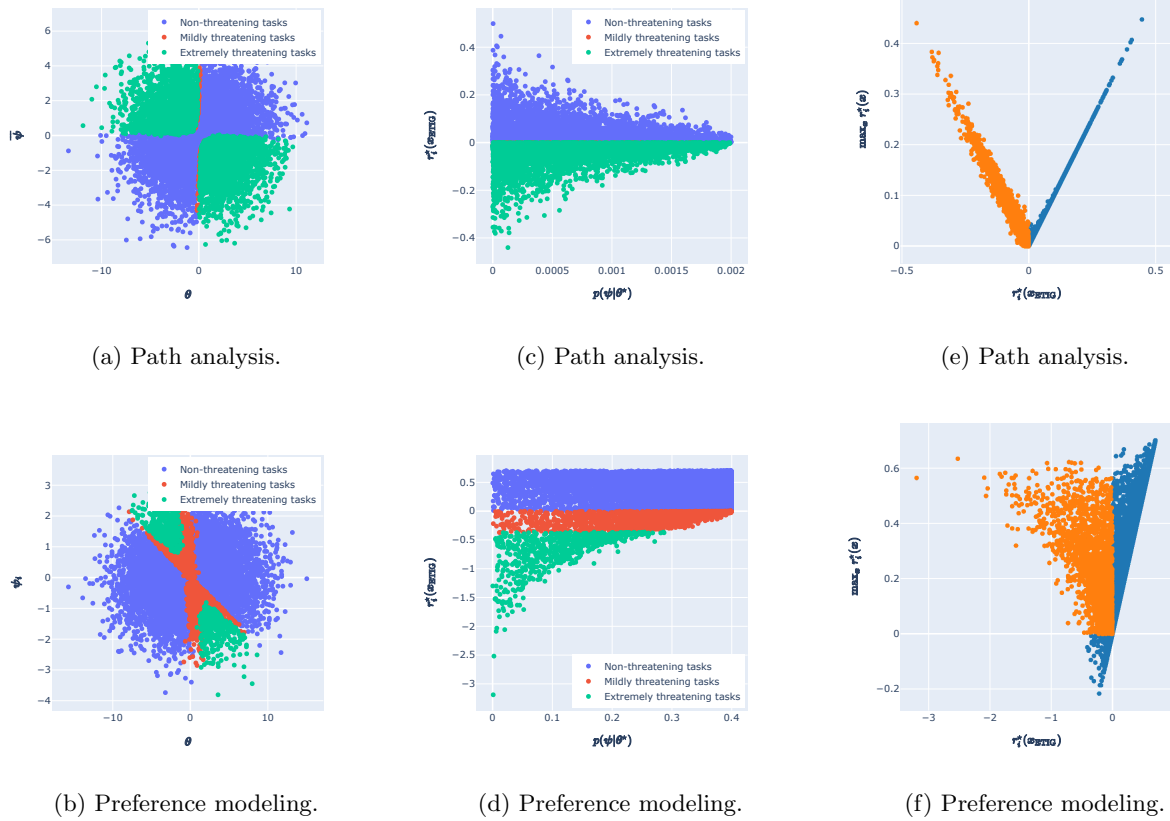


Figure 2: **(a–b)** Presence of threat in the space defined by possible values (θ, ψ) . **(c–d)** $p(\psi|\theta)$ vs. transferable information gain from greedy pursuit of transferable knowledge $(r^{T*}(x_{ETIG}))$. **(e–f)** Transferable information gain from greedy pursuit of transferable knowledge $(r^{T*}(x_{ETIG}))$ vs. maximum achievable transferable information gain $(\max_x r^{T*}(x))$. *Notes.* In all plots, 10,000 parameter values are drawn from the learner’s prior. For the path analysis setting, when ψ is plotted (y -axis in Figure 2a and x -axis in Figure 2c), this is $\frac{\psi_1 + \psi_2 + \psi_3}{3}$.

Prior misspecification in interactive learning. As discussed in Section 3, our theoretical results generalize to analysis of average performance across tasks in the presence of possible prior misspecification. Our work is thus closely related to work on the performance of other Bayesian decision-making algorithms in the presence of prior misspecification (Simchowitz et al., 2021). While Simchowitz et al. (2021) consider the exploration–exploitation dilemma, where the learner trades off seeking information with reward maximization, we consider the trade-off between seeking information about the transferable vs. task-specific parameters. Although prior work has provided some theoretical results on the effect of prior misspecification on active learning (Cuong et al., 2016) and approaches to address it (Go and Isaac, 2022), they do not consider the meta-learning setting, which is the focus of our paper.

sOED for embedded models. The more general setting of targeting inference at a subset of the parameters is referred to as estimation in the presence of nuisance parameters (Foster et al., 2019) or of an embedded model (Rainforth et al., 2023). Acquisition functions that have the same form as the ETIG have been used for model selection (Cavagnaro et al., 2010) and Bayesian optimization (Wang and Jegelka, 2017).

In the context of **model selection**, Ray et al. (2013) showed that naïve sOED can exhibit suboptimal sample efficiency. Sloman et al. (2023) showed that misspecified parameter distributions can lead inference to favor the wrong model in early trials, and discussed the resulting model selection/parameter estimation

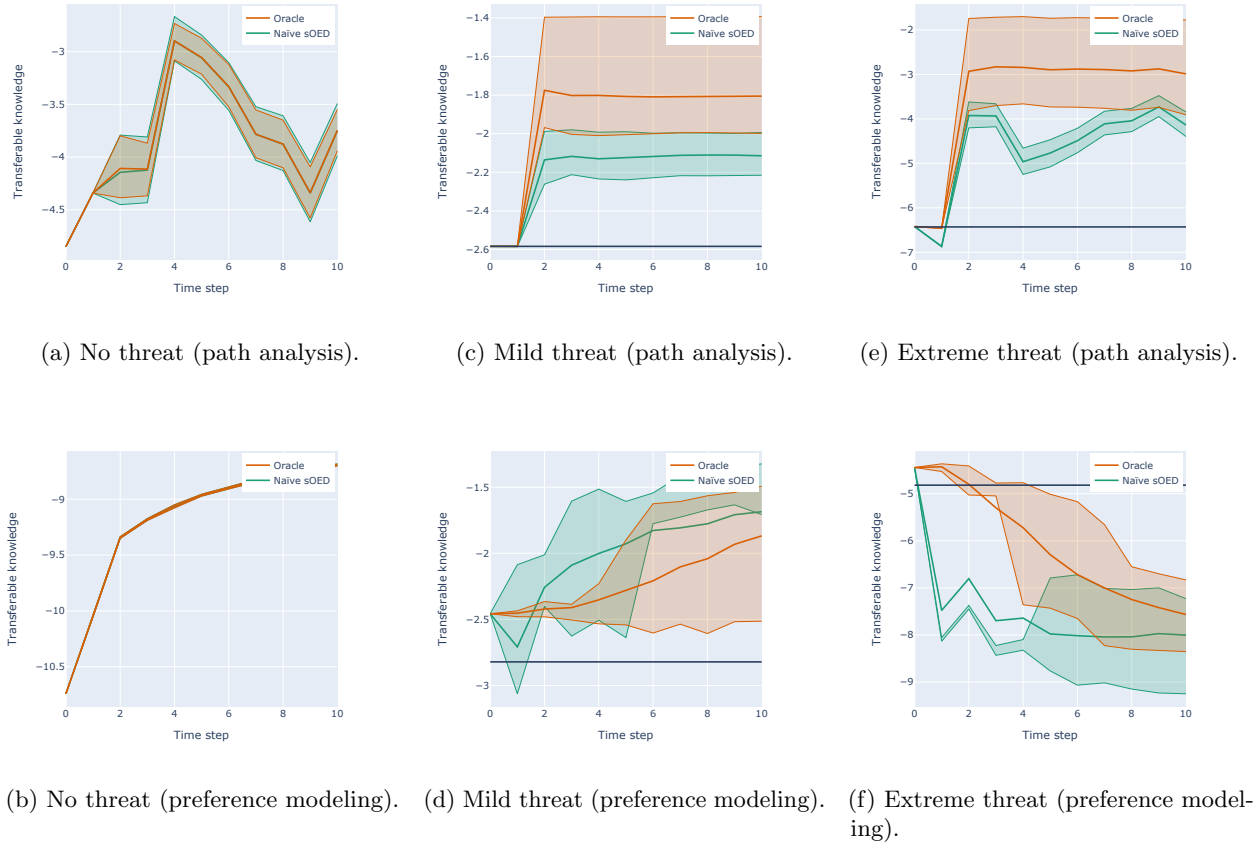


Figure 3: Simulated experiments run under a set of parameter values that fall at each threat level. The x -axes show the time step t . The y -axes are the learner’s degree of transferable knowledge, measured as $\log(p(\theta^*|y(:t), x(:t)))$, i.e., on the basis of all the data seen so far. Solid lines denote the means and shaded regions denote the interquartile ranges across 200 simulated experiments. (c–d) The horizontal line denotes the lower bound of $\mathbb{E}[\log(p(\theta^*|y(0), x(0)))]$ computed on the basis of Theorem 3.8. (e–f) The horizontal line denotes the upper bound of $\mathbb{E}[\log(p(\theta^*|y(0), x(0)))]$ computed on the basis of Theorem 3.8. (Notice that this bound applies only to information gained from $(y(0), x(0))$ and can be exceeded as the learner collects additional data.)

dilemma. Past work has navigated this dilemma via an acquisition function that captures information gain across the joint distribution of model and parameter values (Borth, 1975) and alternating between maximizing information gain about the parameter values and model indicator (Cavagnaro et al., 2016).

Bayesian optimization (BO) can also be seen as an application of sOED where the parameter of interest is the location of the function maximum (Hernández-Lobato et al., 2014; Foster, 2021). Prior work has investigated the limitations of greedy acquisition functions for BO (González et al., 2016) and shown that their performance can be threatened by prior misspecification (Schulz et al., 2016).

6 CONCLUSION

We investigated the application of sOED to the problem of meta-learning. By leveraging the precise measures of information gain offered by the sOED framework, we studied the phenomenon of negative transfer, and showed that task identification protects against negative transfer. The meta-learning dilemma captures the trade-off the active meta-learner faces between acquiring transferable knowledge and task identification. The

conceptual framework, theoretical results, and diagnostic tools our work provides can be applied broadly to the development of robust algorithms for deployment across multiple diverse, but related, environments.

Experimental design objectives (here, parameter estimation) are usually thought of as exploration objectives: better parameter estimates help the learner anticipate the consequences of their subsequent actions. Our work revealed that in the meta-learning context the exploration objective contains a dilemma in and of itself: between exploration for transferable and task-specific information. A natural application of our results is in contexts where Bayesian active meta-learning is performed in service of maximizing another objective (such as contextual BO (Ivanova et al., 2023) or contextual bandits (Simchowitz et al., 2021)). This learner would face a “trilemma” between exploitation, exploration for transferable information and task identification.

Limitations and future work. Our setup imposed some restrictions on the meta-learner. For example, we assumed they have access to the partition between transferable and task-specific parameters, and care exclusively about transferable knowledge acquisition. Finally, while our work has exposed and analyzed a dilemma inherent to the problem of active meta-learning, how to resolve this dilemma still remains an open problem. Future development of active meta-learning algorithms that can successfully navigate the meta-learning dilemma is critical for successful deployment of such algorithms “in the wild.”

Acknowledgements

The authors thank Stephen Menary and Thomas Quilter for helpful discussions, and Xiaomei Mi, Elena Shaw and Amir Sonee for their comments on writing. SJS and SK were supported by the UKRI Turing AI World-Leading Researcher Fellowship, [EP/W002973/1]. AB was supported by the Academy of Finland Flagship programme: Finnish Center for Artificial Intelligence FCAI.

References

Almaatouq, A., Griffiths, T. L., Suchow, J. W., Whiting, M. E., Evans, J., and Watts, D. J. (2022). Beyond playing 20 questions with nature: Integrative experiment design in the social and behavioral sciences. *Behavioral and Brain Sciences*.

Borth, D. M. (1975). A total entropy criterion for the dual problem of model discrimination and parameter estimation. *Journal of the Royal Statistical Society: Statistical Methodology*, 37.

Cavagnaro, D. R., Aranovich, G. J., McClure, S. M., Pitt, M. A., and Myung, J. I. (2016). On the functional form of temporal discounting: An optimized adaptive test. *Journal of Risk and Uncertainty*, 52.

Cavagnaro, D. R., Myung, J. I., Pitt, M. A., and Kujala, J. V. (2010). Adaptive design optimization: A mutual information-based approach to model discrimination in cognitive science. *Neural Computation*, 22.

Chaloner, K. and Verdinelli, I. (1995). Bayesian experimental design: A review. *Statistical Science*, 10(3).

Cuong, N. V., Ye, N., and Lee, W. S. (2016). Robustness of bayesian pool-based active learning against prior misspecification. In *Proceedings of the Thirtieth AAAI Conference on Artificial Intelligence (AAAI-16)*.

Foster, A., Jankowiak, M., Bingham, E., Horsfall, P., Teh, Y. W., Rainforth, T., and Goodman, N. (2019). Variational bayesian optimal experimental design. In *Advances in Neural Information Processing Systems 33 (NeurIPS 2019)*.

Foster, A., Jankowiak, M., O’Meara, M., Teh, Y. W., and Rainforth, T. (2020). A unified stochastic gradient approach to designing bayesian-optimal experiments. In *Proceedings of the Twenty Third International Conference on Artificial Intelligence and Statistics (AISTATS 2020)*.

Foster, A. E. (2021). *Variational, Monte Carlo and Policy-Based Approaches to Bayesian Experimental Design*. PhD thesis, University of Oxford.

Go, J. and Isaac, T. (2022). Robust expected information gain for optimal bayesian experimental design using ambiguity sets. In *Proceedings of the Thirty-Eighth Conference on Uncertainty in Artificial Intelligence (UAI 2022)*.

González, J., Osborne, M., and Lawrence, N. D. (2016). Glasses: Relieving the myopia of bayesian optimisation. In *Proceedings of the Nineteenth International Conference on Artificial Intelligence and Statistics (AISTATS 2016)*.

Griffith, S., Subramanian, K., Scholz, J., Isbell, C. L., and Thomaz, A. L. (2013). Policy shaping: Integrating human feedback with reinforcement learning. In *Advances in Neural Information Processing Systems 26 (NIPS 2013)*.

Hernández-Lobato, J. M., Hoffman, M. W., and Ghahramani, Z. (2014). Predictive entropy search for efficient global optimization of black-box functions. In *Advances in Neural Information Processing Systems 27 (NIPS 2014)*.

Ivanova, D. R., Jennings, J., Rainforth, T., Zhang, C., and Foster, A. (2023). Co-bed: Information-theoretic contextual optimization via bayesian experimental design. In *Proceedings of the 40th International Conference on Machine Learning (ICML 2023)*.

Javed, K. and White, M. (2019). Meta-learning representations for continual learning. In *Advances in Neural Information Processing Systems 32 (NeurIPS 2019)*.

Krefeld-Schwalb, A., Pachur, T., and Scheibehenne, B. (2022). Structural parameter interdependencies in computational models of cognition. *Psychological Review*, 129(2).

Kveton, B., Konobeev, M., Zaheer, M., Hsu, C.-W., Mladenov, M., Boutilier, C., and Szepesvari, C. (2021). Meta-thompson sampling. In *Proceedings of the 38th International Conference on Machine Learning (ICML 2021)*.

Mehta, V., Paria, B., Schneider, J., Ermon, S., and Neiswanger, W. (2022). An experimental design perspective on model-based reinforcement learning. In *The Tenth International Conference on Learning Representations (ICLR 2022)*.

Paninski, L. (2005). Asymptotic theory of information-theoretic experimental design. *Neural Computation*, 17.

Peng, Z., Zhang, W., Han, N., Fang, X., Kang, P., and Teng, L. (2020). Active transfer learning. In *IEEE Transactions on Circuits and Systems for Video Technology*.

Rainforth, T., Cornish, R., Yang, H., Warrington, A., and Wood, F. (2018). On nesting monte carlo estimators. In *Proceedings of the 35th International Conference on Machine Learning (ICML 2018)*.

Rainforth, T., Foster, A., Ivanova, D. R., and Smith, F. B. (2023). Modern bayesian experimental design. <https://arxiv.org/abs/2302.14545>.

Ray, D., Golovin, D., Krause, A., and Camerer, C. (2013). Bayesian rapid optimal adaptive design (broad): Method and application distinguishing models of risky choice. Unpublished manuscript.

Ryan, E. G., Drovandi, C. C., McGree, J. M., and Pettitt, A. N. (2016). A review of modern computational algorithms for bayesian optimal design. *International Statistical Review*, 84(1).

Ryan, E. G., Drovandi, C. C., and Pettitt, A. N. (2015). Fully bayesian experimental design for pharmacokinetic studies. *Entropy*, 17.

Schulz, E., Speekenbrink, M., Hernández-Lobato, J. M., Ghahramani, Z., and Gershman, S. J. (2016). Quantifying mismatch in bayesian optimization. In *NIPS Workshop on Bayesian Optimization*.

Senarathne, S. G. J., Drovandi, C. C., and McGree, J. M. (2020). A laplace-based algorithm for bayesian adaptive design. *Statistics and Computing*, 30.

Simchowitz, M., Tosh, C., Krishnamurthy, A., Hsu, D., Lykouris, T., Dudík, M., and Schapire, R. (2021). Bayesian decision-making under misspecified priors with applications to meta-learning. In *Advances in Neural Information Processing Systems 35 (NeurIPS 2021)*.

Sloman, S. J. (2022). *Towards robust Bayesian adaptive design methods for the study of human behavior*. PhD thesis, Carnegie Mellon University.

Sloman, S. J., Cavagnaro, D., and Broomell, S. B. (2023). Knowing what to know: Implications of the choice of prior distribution on the behavior of adaptive design optimization. <https://arxiv.org/abs/2303.12683>.

Sugiyama, M., Rubens, N., and Müller, K.-R. (2008). A conditional expectation approach to model selection and active learning under covariate shift. In *Dataset Shift in Machine Learning*. MIT Press.

Wang, Z., Dai, Z., Poczos, B., and Carbonell, J. (2019). Characterizing and avoiding negative transfer. In *Proceedings of the IEEE/CVF Conference on Computer Vision and Pattern Recognition (CVPR)*.

Wang, Z. and Jegelka, S. (2017). Max-value entropy search for efficient bayesian optimization. In *Proceedings of the 34th International Conference on Machine Learning (ICML 2017)*.

Zhao, E., Liu, A., Anandkumar, A., and Yue, Y. (2021). Active learning under label shift. In *Proceedings of the Twenty Fourth International Conference on Artificial Intelligence and Statistics (AISTATS 2021)*.

Supplementary Materials

The appendix is organized as follows:

- In Appendix A, we provide proofs of all our mathematical results.
- In Appendix B, we provide a simple example demonstrating that maximizing ETIG can be at odds with maximizing ETSIG.
- In Appendix C, we provide details of the experiments presented in Section 4.

A PROOFS OF MATHEMATICAL RESULTS

A.1 Definitions

- $D_{KL}(Q \parallel P)$ is the Kullback-Leibler divergence from Q to P :

$$D_{KL}(Q \parallel P) = \int_{\mathcal{Y}} \log \frac{q(\mathbf{y})}{p(\mathbf{y})} q(\mathbf{y}) d\mathbf{y}$$

- $H(Q \parallel P)$ is the cross-entropy from Q to P :

$$H(Q \parallel P) = - \int_{\mathcal{Y}} \log(p(\mathbf{y})) q(\mathbf{y}) d\mathbf{y}$$

- $H(Q)$ is the entropy of distribution Q :

$$H(Q) = - \int_{\mathcal{Y}} \log(q(\mathbf{y})) q(\mathbf{y}) d\mathbf{y}$$

A.2 Generalized misjudgments and notation

As stated in Section 3, our proofs consider generalized misjudgments (Definition 3.3). For this, we require the following additional notation.

$Q_{\Psi|\theta^*}$ refers to the “true” distribution of Ψ , and Q refers to distributions induced by $Q_{\Psi|\theta^*}$, subscripted to indicate the corresponding random variable. We denote the associated density function by q . For example, the “true” outcome distribution is $Q_{Y|x,\theta^*}$, where for any \mathbf{y} , $q(\mathbf{y}|\mathbf{x}) = \mathbb{E}_{\psi \sim Q_{\Psi|\theta^*}} [q(\mathbf{y}|\mathbf{x}, \theta^*, \psi)]$.

When results are presented in the main text, they are for the special case where $Q_{\Psi|\theta^*} = \delta(\psi^*)$ (the Dirac delta at ψ^*). This appendix also presents the generalized statements of our theorems.

We also use $\mathcal{M}_L(\mathbf{x}, \theta)$, $\mathcal{M}_{\text{pred}}(\mathbf{x})$ and $\tilde{\mathcal{M}}_{\text{pred}}(\mathbf{x})$ to mean the following generalized versions of the corresponding definitions in the main text:

$$\mathcal{M}_L(\mathbf{x}, \theta) = D_{KL}(Q_{Y|x,\theta^*} \parallel P_{Y|x,\theta}) \tag{4}$$

$$\mathcal{M}_{\text{pred}}(\mathbf{x}) = D_{KL}(Q_{Y|x,\theta^*} \parallel P_{Y|x}) \tag{5}$$

$$\tilde{\mathcal{M}}_{\text{pred}}(\mathbf{x}) = D_{KL}(Q_{Y|x,\theta^*} \parallel \tilde{P}_{Y|x}) \tag{6}$$

A.3 Generalized statement and derivation of Proposition 3.2

Proposition 3.2* (Decomposition of r^{T*}).

$$r^{T*}(\mathbf{x}) = \underbrace{D_{KL}(Q_{Y|x,\theta^*} \parallel P_{Y|x})}_{\mathcal{M}_{\text{pred}}(\mathbf{x})} - \underbrace{D_{KL}(Q_{Y|x,\theta^*} \parallel P_{Y|x,\theta^*})}_{\mathcal{M}_L^*(\mathbf{x})}$$

Proposition 3.2* states that $r^{T*}(\mathbf{x})$, the transferable information the learner will gain in expectation in a set of tasks characterized by θ^* and $Q_{\Psi|\theta^*}$, is positively related to $\mathcal{M}_{\text{pred}}(\mathbf{x})$ (how much the actual outcome distribution differs from the learner’s expected outcome distribution) and negatively related to $\mathcal{M}_L^*(\mathbf{x})$ (the extent of the learner’s misjudgment of the likelihood function under θ^*).

Derivation of Proposition 3.2*.

$$\begin{aligned}
r^{T*}(\mathbf{x}) &= \mathbb{E}_{\mathbf{y} \sim Q_{\mathbf{Y}|\mathbf{x}, \boldsymbol{\theta}^*}} \left[\log \frac{p(\mathbf{y}|\mathbf{x}, \boldsymbol{\theta}^*)}{p(\mathbf{y}|\mathbf{x})} \right] \\
&= H(Q_{\mathbf{Y}|\mathbf{x}, \boldsymbol{\theta}^*} \parallel P_{\mathbf{Y}|\mathbf{x}}) - H(Q_{\mathbf{Y}|\mathbf{x}, \boldsymbol{\theta}^*} \parallel P_{\mathbf{Y}|\mathbf{x}, \boldsymbol{\theta}^*}) \\
&= H(Q_{\mathbf{Y}|\mathbf{x}, \boldsymbol{\theta}^*}) + D_{KL}(Q_{\mathbf{Y}|\mathbf{x}, \boldsymbol{\theta}^*} \parallel P_{\mathbf{Y}|\mathbf{x}}) - H(Q_{\mathbf{Y}|\mathbf{x}, \boldsymbol{\theta}^*}) - D_{KL}(Q_{\mathbf{Y}|\mathbf{x}, \boldsymbol{\theta}^*} \parallel P_{\mathbf{Y}|\mathbf{x}, \boldsymbol{\theta}^*}) \\
&= D_{KL}(Q_{\mathbf{Y}|\mathbf{x}, \boldsymbol{\theta}^*} \parallel P_{\mathbf{Y}|\mathbf{x}}) - D_{KL}(Q_{\mathbf{Y}|\mathbf{x}, \boldsymbol{\theta}^*} \parallel P_{\mathbf{Y}|\mathbf{x}, \boldsymbol{\theta}^*})
\end{aligned} \tag{7}$$

A.4 Generalized statement and proof of Theorem 3.8

Theorem 3.8* (Bounds as a function of threat level). *Consider possible distributions Q_{Ψ} from some distribution class, and a parameter ϕ that smoothly indexes distributions from that class. We here establish bounds for $r^{T*}(\mathbf{x})$ with respect to ϕ .*

Given $\boldsymbol{\theta}^*$, $Q_{\Psi|\boldsymbol{\theta}^*}$ and ϵ that satisfies Assumption 3.7, $r^{T*}(\mathbf{x})$ is generally upper-bounded as

$$r^{T*}(\mathbf{x}) \leq \left(\int_{\mathcal{T} \setminus N_{\epsilon}(\boldsymbol{\theta}^*)} p(\boldsymbol{\theta}) d\boldsymbol{\theta} \right) (\tilde{\mathcal{M}}_{\text{pred}}(\mathbf{x}) - \mathcal{M}_L^*(\mathbf{x}))$$

Under the same conditions, $r^{T*}(\mathbf{x})$ is additionally bounded as follows for each threat level:

1. In the presence of **no threat**, $r^{T*}(\mathbf{x}) \geq 0$.
2. In the presence of **mild threat**, $r^{T*}(\mathbf{x}) < 0$ and $r^{T*}(\mathbf{x}) \geq \mathcal{M}_{\text{pred}}(\mathbf{x}) - \mathbb{E}_{\boldsymbol{\theta} \sim P_{\Theta}} [\mathcal{M}_L(\mathbf{x}, \boldsymbol{\theta})]$.
3. In the presence of **extreme threat**, $r^{T*}(\mathbf{x}) < \mathcal{M}_{\text{pred}}(\mathbf{x}) - \mathbb{E}_{\boldsymbol{\theta} \sim P_{\Theta}} [\mathcal{M}_L(\mathbf{x}, \boldsymbol{\theta})]$. In addition, if $\exists \tilde{\phi}$ such that $\forall \phi < \tilde{\phi}$ or $\forall \phi > \tilde{\phi}$ the following conditions hold:
 - (a) the distribution indexed by ϕ is a member of the considered distribution class, and
 - (b) if $\phi > \tilde{\phi}$, $\frac{\partial \mathcal{M}_L^*(\mathbf{x})}{\partial \phi} > \frac{\partial \tilde{\mathcal{M}}_{\text{pred}}(\mathbf{x})}{\partial \phi}$ when the derivatives are evaluated at ϕ ; else if $\phi < \tilde{\phi}$, $\frac{\partial \mathcal{M}_L^*(\mathbf{x})}{\partial \phi} < \frac{\partial \tilde{\mathcal{M}}_{\text{pred}}(\mathbf{x})}{\partial \phi}$ when the derivatives are evaluated at ϕ ,

we can say that $r^{T*}(\mathbf{x})$ is unbounded below in the sense that $\forall C \in \mathbb{R}$, $\exists \phi$ such that when Q_{Ψ} is indexed by ϕ , $r^{T*}(\mathbf{x}) < C$.

Theorem 3.8 states Theorem 3.8* in the special case where the class of distributions is the set of delta functions $\delta(\phi)$.

Note on discrete transferable parameter spaces. Results that rely on Assumption 3.7 also apply in case $\boldsymbol{\theta}$ can only take finitely many values. The proofs proceed exactly the same, with the exception that $N_{\epsilon}(\boldsymbol{\theta})$ is redefined to be simply the singleton $\{\boldsymbol{\theta}\}$.

The proof of Theorem 3.8* depends on the following lemmas:

Lemma A.1 gives an upper bound on $\mathcal{M}_{\text{pred}}(\mathbf{x})$ in terms of $\mathcal{M}_L^*(\mathbf{x})$.

Lemma A.1 ($\mathcal{M}_{\text{pred}}(\mathbf{x})$ upper bound in terms of $\mathcal{M}_L^*(\mathbf{x})$). *Under Assumption 3.7, $\mathcal{M}_{\text{pred}}(\mathbf{x})$ is upper-bounded as follows:*

$$\mathcal{M}_{\text{pred}}(\mathbf{x}) \leq \left(\int_{N_{\epsilon}(\boldsymbol{\theta}^*)} p(\boldsymbol{\theta}) d\boldsymbol{\theta} \right) \mathcal{M}_L^*(\mathbf{x}) + \left(\int_{\mathcal{T} \setminus N_{\epsilon}(\boldsymbol{\theta}^*)} p(\boldsymbol{\theta}) d\boldsymbol{\theta} \right) \tilde{\mathcal{M}}_{\text{pred}}(\mathbf{x})$$

Lemma A.2 gives another upper bound on $\mathcal{M}_L(\mathbf{x}, \boldsymbol{\theta})$ in terms of $\mathbb{E}_{\boldsymbol{\theta} \sim P_{\Theta}} [\mathcal{M}_L(\mathbf{x}, \boldsymbol{\theta})]$, which is required for analysis of mild and extreme threat. Lemma A.2 also establishes that the three threat levels are mutually exclusive.

Lemma A.2 ($\mathcal{M}_{\text{pred}}(\mathbf{x}) \leq \mathbb{E}_{\boldsymbol{\theta} \sim P_{\boldsymbol{\Theta}}} [\mathcal{M}_L(\mathbf{x}, \boldsymbol{\theta})]$).

$$\mathcal{M}_{\text{pred}}(\mathbf{x}) \leq \mathbb{E}_{\boldsymbol{\theta} \sim P_{\boldsymbol{\Theta}}} [\mathcal{M}_L(\mathbf{x}, \boldsymbol{\theta})]$$

Proof of Lemma A.1.

$$\begin{aligned}
\mathcal{M}_{\text{pred}}(\mathbf{x}) &= D_{\text{KL}}(Q_{\mathbf{Y}|\mathbf{x}, \boldsymbol{\theta}^*} \parallel P_{\mathbf{Y}|\mathbf{x}}) && \text{(Proposition 3.2*)} \\
&= \int_{\mathcal{Y}} \log \frac{q(\mathbf{y}|\mathbf{x}, \boldsymbol{\theta}^*)}{p(\mathbf{y}|\mathbf{x})} q(\mathbf{y}|\mathbf{x}, \boldsymbol{\theta}^*) d\mathbf{y} \\
&= \int_{\mathcal{Y}} (\log(q(\mathbf{y}|\mathbf{x}, \boldsymbol{\theta}^*)) - \log(p(\mathbf{y}|\mathbf{x}))) q(\mathbf{y}|\mathbf{x}, \boldsymbol{\theta}^*) d\mathbf{y} \\
&\leq \int_{\mathcal{Y}} \left(\log q(\mathbf{y}|\mathbf{x}, \boldsymbol{\theta}^*) - \left(\int_{N_{\epsilon}(\boldsymbol{\theta}^*)} p(\boldsymbol{\theta}) d\boldsymbol{\theta} \right) \log(p(\mathbf{y}|\mathbf{x}, \boldsymbol{\theta}^*)) - \left(\int_{\mathcal{T} \setminus N_{\epsilon}(\boldsymbol{\theta}^*)} p(\boldsymbol{\theta}) d\boldsymbol{\theta} \right) \log \tilde{p}(\mathbf{y}|\mathbf{x}) \right) q(\mathbf{y}|\mathbf{x}, \boldsymbol{\theta}^*) d\mathbf{y} && \text{(Assumption 3.7)} \\
&= -H(Q_{\mathbf{Y}|\mathbf{x}, \boldsymbol{\theta}^*}) + \left(\int_{N_{\epsilon}(\boldsymbol{\theta}^*)} p(\boldsymbol{\theta}) d\boldsymbol{\theta} \right) H(Q_{\mathbf{Y}|\mathbf{x}, \boldsymbol{\theta}^*} \parallel P_{\mathbf{Y}|\mathbf{x}, \boldsymbol{\theta}^*}) + \left(\int_{\mathcal{T} \setminus N_{\epsilon}(\boldsymbol{\theta}^*)} p(\boldsymbol{\theta}) d\boldsymbol{\theta} \right) H(Q_{\mathbf{Y}|\mathbf{x}, \boldsymbol{\theta}^*} \parallel \tilde{P}_{\mathbf{Y}|\mathbf{x}}) \\
&= -H(Q_{\mathbf{Y}|\mathbf{x}, \boldsymbol{\theta}^*}) + \left(\int_{N_{\epsilon}(\boldsymbol{\theta}^*)} p(\boldsymbol{\theta}) d\boldsymbol{\theta} \right) (H(Q_{\mathbf{Y}|\mathbf{x}, \boldsymbol{\theta}^*}) + D_{\text{KL}}(Q_{\mathbf{Y}|\mathbf{x}, \boldsymbol{\theta}^*} \parallel P_{\mathbf{Y}|\mathbf{x}, \boldsymbol{\theta}^*})) \\
&\quad + \left(\int_{\mathcal{T} \setminus N_{\epsilon}(\boldsymbol{\theta}^*)} p(\boldsymbol{\theta}) d\boldsymbol{\theta} \right) (H(Q_{\mathbf{Y}|\mathbf{x}, \boldsymbol{\theta}^*}) + D_{\text{KL}}(Q_{\mathbf{Y}|\mathbf{x}, \boldsymbol{\theta}^*} \parallel \tilde{P}_{\mathbf{Y}|\mathbf{x}})) \\
&= \left(\int_{N_{\epsilon}(\boldsymbol{\theta}^*)} p(\boldsymbol{\theta}) d\boldsymbol{\theta} \right) D_{\text{KL}}(Q_{\mathbf{Y}|\mathbf{x}, \boldsymbol{\theta}^*} \parallel P_{\mathbf{Y}|\mathbf{x}, \boldsymbol{\theta}^*}) + \left(\int_{\mathcal{T} \setminus N_{\epsilon}(\boldsymbol{\theta}^*)} p(\boldsymbol{\theta}) d\boldsymbol{\theta} \right) D_{\text{KL}}(Q_{\mathbf{Y}|\mathbf{x}, \boldsymbol{\theta}^*} \parallel \tilde{P}_{\mathbf{Y}|\mathbf{x}}) \\
&= \left(\int_{N_{\epsilon}(\boldsymbol{\theta}^*)} p(\boldsymbol{\theta}) d\boldsymbol{\theta} \right) \mathcal{M}_L^*(\mathbf{x}) + \left(\int_{\mathcal{T} \setminus N_{\epsilon}(\boldsymbol{\theta}^*)} p(\boldsymbol{\theta}) d\boldsymbol{\theta} \right) \tilde{\mathcal{M}}_{\text{pred}}(\mathbf{x}) && (8)
\end{aligned}$$

Proof of Lemma A.2.

$$\begin{aligned}
\mathcal{M}_{\text{pred}}(\mathbf{x}) - \mathbb{E}_{\boldsymbol{\theta} \sim P_{\boldsymbol{\Theta}}} [\mathcal{M}_L(\mathbf{x}, \boldsymbol{\theta})] &= D_{\text{KL}}(Q_{\mathbf{Y}|\mathbf{x}, \boldsymbol{\theta}^*} \parallel P_{\mathbf{Y}|\mathbf{x}}) - \mathbb{E}_{\boldsymbol{\theta} \sim P_{\boldsymbol{\Theta}}} [D_{\text{KL}}(Q_{\mathbf{Y}|\mathbf{x}, \boldsymbol{\theta}^*} \parallel P_{\mathbf{Y}|\mathbf{x}, \boldsymbol{\theta}})] \\
&= H(Q_{\mathbf{Y}|\mathbf{x}, \boldsymbol{\theta}^*}) + D_{\text{KL}}(Q_{\mathbf{Y}|\mathbf{x}, \boldsymbol{\theta}^*} \parallel P_{\mathbf{Y}|\mathbf{x}}) - H(Q_{\mathbf{Y}|\mathbf{x}, \boldsymbol{\theta}^*}) - \mathbb{E}_{\boldsymbol{\theta} \sim P_{\boldsymbol{\Theta}}} [D_{\text{KL}}(Q_{\mathbf{Y}|\mathbf{x}, \boldsymbol{\theta}^*} \parallel P_{\mathbf{Y}|\mathbf{x}, \boldsymbol{\theta}})] \\
&= H(Q_{\mathbf{Y}|\mathbf{x}, \boldsymbol{\theta}^*} \parallel P_{\mathbf{Y}|\mathbf{x}}) - \mathbb{E}_{\boldsymbol{\theta} \sim P_{\boldsymbol{\Theta}}} [H(Q_{\mathbf{Y}|\mathbf{x}, \boldsymbol{\theta}^*} \parallel P_{\mathbf{Y}|\mathbf{x}, \boldsymbol{\theta}})] \\
&= -\mathbb{E}_{\boldsymbol{\theta} \sim P_{\boldsymbol{\Theta}}} [-H(Q_{\mathbf{Y}|\mathbf{x}, \boldsymbol{\theta}^*} \parallel P_{\mathbf{Y}|\mathbf{x}}) + H(Q_{\mathbf{Y}|\mathbf{x}, \boldsymbol{\theta}^*} \parallel P_{\mathbf{Y}|\mathbf{x}, \boldsymbol{\theta}})] \\
&= -\mathbb{E}_{\boldsymbol{\theta} \sim P_{\boldsymbol{\Theta}}} \left[\mathbb{E}_{\mathbf{y} \sim Q_{\mathbf{Y}|\mathbf{x}, \boldsymbol{\theta}^*}} [\log(p(\mathbf{y}|\mathbf{x})) - \log(p(\mathbf{y}|\mathbf{x}, \boldsymbol{\theta}))] \right] \\
&= -\mathbb{E}_{\mathbf{y} \sim Q_{\mathbf{Y}|\mathbf{x}, \boldsymbol{\theta}^*}} \left[\log(p(\mathbf{y}|\mathbf{x})) - \mathbb{E}_{\boldsymbol{\theta} \sim P_{\boldsymbol{\Theta}}} [\log(p(\mathbf{y}|\mathbf{x}, \boldsymbol{\theta}))] \right] \\
&\leq -\mathbb{E}_{\mathbf{y} \sim Q_{\mathbf{Y}|\mathbf{x}, \boldsymbol{\theta}^*}} \left[\log(p(\mathbf{y}|\mathbf{x})) - \log \left(\mathbb{E}_{\boldsymbol{\theta} \sim P_{\boldsymbol{\Theta}}} [p(\mathbf{y}|\mathbf{x}, \boldsymbol{\theta})] \right) \right] && \text{(Jensen's inequality)} \\
&= -\mathbb{E}_{\mathbf{y} \sim Q_{\mathbf{Y}|\mathbf{x}, \boldsymbol{\theta}^*}} [\log(p(\mathbf{y}|\mathbf{x})) - \log(p(\mathbf{y}|\mathbf{x}))] \\
&= 0 && (9)
\end{aligned}$$

Proof of generic upper bound.

$$\begin{aligned}
r^{T*}(\mathbf{x}) &\leq \left(\int_{N_\epsilon(\boldsymbol{\theta}^*)} p(\boldsymbol{\theta}) d\boldsymbol{\theta} \right) \mathcal{M}_L^*(\mathbf{x}) + \left(\int_{\mathcal{T} \setminus N_\epsilon(\boldsymbol{\theta}^*)} p(\boldsymbol{\theta}) d\boldsymbol{\theta} \right) \tilde{\mathcal{M}}_{\text{pred}}(\mathbf{x}) - \mathcal{M}_L^*(\mathbf{x}) \quad (\text{Lemma A.1}) \\
&= \left(\int_{\mathcal{T} \setminus N_\epsilon(\boldsymbol{\theta}^*)} p(\boldsymbol{\theta}) d\boldsymbol{\theta} \right) (\tilde{\mathcal{M}}_{\text{pred}}(\mathbf{x}) - \mathcal{M}_L^*(\mathbf{x}))
\end{aligned} \tag{10}$$

Bounds in the presence of no threat ($\mathcal{M}_L^*(\mathbf{x}) \leq \mathcal{M}_{\text{pred}}(\mathbf{x})$). The lower bound of 0 follows directly from Proposition 3.2*.

Bounds in the presence of mild threat ($\mathcal{M}_{\text{pred}}(\mathbf{x}) < \mathcal{M}_L^*(\mathbf{x}) \leq \mathbb{E}_{\boldsymbol{\theta} \sim P_{\boldsymbol{\Theta}}} [\mathcal{M}_L(\mathbf{x}, \boldsymbol{\theta})]$). The lower bound of $r^{T*}(\mathbf{x})$ is achieved when $\mathcal{M}_L^*(\mathbf{x}) = \mathbb{E}_{\boldsymbol{\theta} \sim P_{\boldsymbol{\Theta}}} [\mathcal{M}_L(\mathbf{x}, \boldsymbol{\theta})]$ and follows directly from Proposition 3.2*.

The upper bound on $r^{T*}(\mathbf{x})$ of 0 follows directly from Proposition 3.2*.

Bounds in the presence of extreme threat ($\mathcal{M}_L^*(\mathbf{x}) > \mathbb{E}_{\boldsymbol{\theta} \sim P_{\boldsymbol{\Theta}}} [\mathcal{M}_L(\mathbf{x}, \boldsymbol{\theta})]$). The upper bound is approached as $\mathcal{M}_L^*(\mathbf{x})$ approaches $\mathbb{E}_{\boldsymbol{\theta} \sim P_{\boldsymbol{\Theta}}} [\mathcal{M}_L(\mathbf{x}, \boldsymbol{\theta})]$ and follows directly from Proposition 3.2*.

Conditions (a) and (b) imply that $r^{T*}(\mathbf{x})$ plummets uncontrollably, i.e., can become arbitrarily negative, with the magnitude of ϕ in at least one direction.

If the conditions hold $\forall \phi > \tilde{\phi}$, they imply that $r^{T*}(\mathbf{x})$ can grow arbitrarily negative as $\phi \rightarrow \infty$, or that $r^{T*}(\mathbf{x})$ decreases with ϕ at at least some steady rate:

$$\frac{\partial r^{T*}(\mathbf{x})}{\partial \phi} < -c \quad \forall \phi > \tilde{\phi} \tag{11}$$

for some positive constant c .

We can use the generic upper bound on $r^{T*}(\mathbf{x})$ to bound its derivative with respect to ϕ : $r^{T*}(\mathbf{x})$ must grow more slowly with respect to ϕ than its upper bound by at least some margin, otherwise it would exceed the bound at some value of ϕ . This gives us:

$$\begin{aligned}
\frac{\partial r^{T*}(\mathbf{x})}{\partial \phi} &\leq \frac{\partial \left(\left(\int_{\mathcal{T} \setminus N_\epsilon(\boldsymbol{\theta}^*)} p(\boldsymbol{\theta}) d\boldsymbol{\theta} \right) (\tilde{\mathcal{M}}_{\text{pred}}(\mathbf{x}) - \mathcal{M}_L^*(\mathbf{x})) \right)}{\partial \phi} - c \quad \forall \phi > \tilde{\phi} \\
&= \left(\int_{\mathcal{T} \setminus N_\epsilon(\boldsymbol{\theta}^*)} p(\boldsymbol{\theta}) d\boldsymbol{\theta} \right) \frac{\partial \tilde{\mathcal{M}}_{\text{pred}}(\mathbf{x})}{\partial \phi} - \left(\int_{\mathcal{T} \setminus N_\epsilon(\boldsymbol{\theta}^*)} p(\boldsymbol{\theta}) d\boldsymbol{\theta} \right) \frac{\partial \mathcal{M}_L^*(\mathbf{x})}{\partial \phi} - c \quad \forall \phi > \tilde{\phi}
\end{aligned} \tag{12}$$

Plugging this into Equation (11), we obtain

$$\begin{aligned}
\left(\int_{\mathcal{T} \setminus N_\epsilon(\boldsymbol{\theta}^*)} p(\boldsymbol{\theta}) d\boldsymbol{\theta} \right) \frac{\partial \tilde{\mathcal{M}}_{\text{pred}}(\mathbf{x})}{\partial \phi} - \left(\int_{\mathcal{T} \setminus N_\epsilon(\boldsymbol{\theta}^*)} p(\boldsymbol{\theta}) d\boldsymbol{\theta} \right) \frac{\partial \mathcal{M}_L^*(\mathbf{x})}{\partial \phi} - c &< -c \quad \forall \phi > \tilde{\phi} \\
\frac{\partial \tilde{\mathcal{M}}_{\text{pred}}(\mathbf{x})}{\partial \phi} &< \frac{\partial \mathcal{M}_L^*(\mathbf{x})}{\partial \phi} \quad \forall \phi > \tilde{\phi}
\end{aligned} \tag{13}$$

which is a condition of the theorem.

If the conditions hold $\forall \phi < \tilde{\phi}$, they imply that $r^{T*}(\mathbf{x})$ can grow arbitrarily negative as $\phi \rightarrow -\infty$, or that $r^{T*}(\mathbf{x})$ increases with ϕ at at least some steady rate:

$$\frac{\partial r^{T*}(\mathbf{x})}{\partial \phi} > c \quad \forall \phi < \tilde{\phi} \tag{14}$$

Using the same logic as above, we can lower bound $\frac{\partial r^{T*}(\mathbf{x})}{\partial \phi}$: $r^{T*}(\mathbf{x})$ must grow more slowly with respect

to $-\phi$ (i.e., more quickly with respect to ϕ) than its upper bound by at least some margin. This gives us:

$$\begin{aligned} \frac{\partial r^{\text{T}\star}(\mathbf{x})}{\partial \phi} &\geq \frac{\partial \left(\left(\int_{\mathcal{T} \setminus N_{\epsilon}(\boldsymbol{\theta}^*)} p(\boldsymbol{\theta}) d\boldsymbol{\theta} \right) \left(\tilde{\mathcal{M}}_{\text{pred}}(\mathbf{x}) - \mathcal{M}_L^{\star}(\mathbf{x}) \right) \right)}{\partial \phi} + c \quad \forall \phi < \tilde{\phi} \\ &= \left(\int_{\mathcal{T} \setminus N_{\epsilon}(\boldsymbol{\theta}^*)} p(\boldsymbol{\theta}) d\boldsymbol{\theta} \right) \frac{\partial \tilde{\mathcal{M}}_{\text{pred}}(\mathbf{x})}{\partial \phi} - \left(\int_{\mathcal{T} \setminus N_{\epsilon}(\boldsymbol{\theta}^*)} p(\boldsymbol{\theta}) d\boldsymbol{\theta} \right) \frac{\partial \mathcal{M}_L^{\star}(\mathbf{x})}{\partial \phi} + c \quad \forall \phi < \tilde{\phi} \quad (15) \end{aligned}$$

Plugging this into Equation (14), we obtain

$$\begin{aligned} \left(\int_{\mathcal{T} \setminus N_{\epsilon}(\boldsymbol{\theta}^*)} p(\boldsymbol{\theta}) d\boldsymbol{\theta} \right) \frac{\partial \tilde{\mathcal{M}}_{\text{pred}}(\mathbf{x})}{\partial \phi} - \left(\int_{\mathcal{T} \setminus N_{\epsilon}(\boldsymbol{\theta}^*)} p(\boldsymbol{\theta}) d\boldsymbol{\theta} \right) \frac{\partial \mathcal{M}_L^{\star}(\mathbf{x})}{\partial \phi} + c &> c \quad \forall \phi < \tilde{\phi} \\ \frac{\partial \tilde{\mathcal{M}}_{\text{pred}}(\mathbf{x})}{\partial \phi} &> \frac{\partial \mathcal{M}_L^{\star}(\mathbf{x})}{\partial \phi} \quad \forall \phi < \tilde{\phi} \quad (16) \end{aligned}$$

which is a condition of the theorem.

A.5 Generalized statement and proof of Theorem 3.9

Theorem 3.9* ($\mathcal{M}_L^{\star}(\mathbf{x})$ decreases with the distance between $P_{\Psi|\boldsymbol{\theta}^*}$ and $Q_{\Psi|\boldsymbol{\theta}^*}$). For any $\alpha \in (0, 1]$, the lower bound on $\mathcal{M}_L^{\star}(\mathbf{x})$ is lower under the distribution $P_{\Psi|\boldsymbol{\theta}^*}^{\star} := \alpha Q_{\Psi|\boldsymbol{\theta}^*} + (1 - \alpha) P_{\Psi|\boldsymbol{\theta}^*}$ than under the prior $P_{\Psi|\boldsymbol{\theta}^*}$.

Proof. Define $p^{\star}(\mathbf{y}|\mathbf{x}, \boldsymbol{\theta}^*)$ as the likelihood of \mathbf{y} under the prior $P_{\Psi|\boldsymbol{\theta}^*}^{\star}$.

$$\begin{aligned} \text{D}_{\text{KL}} \left(Q_{\mathbf{Y}|\mathbf{x}, \boldsymbol{\theta}^*} \parallel P_{\mathbf{Y}|\mathbf{x}, \boldsymbol{\theta}^*}^{\star} \right) &= \int_{\mathcal{Y}} \log \frac{q(\mathbf{y}|\mathbf{x}, \boldsymbol{\theta}^*)}{p^{\star}(\mathbf{y}|\mathbf{x}, \boldsymbol{\theta}^*)} q(\mathbf{y}|\mathbf{x}, \boldsymbol{\theta}^*) d\mathbf{y} \\ &= \int_{\mathcal{Y}} \log \frac{\mathbb{E}_{\boldsymbol{\psi} \sim Q_{\Psi|\boldsymbol{\theta}^*}} [p(\mathbf{y}|\mathbf{x}, \boldsymbol{\theta}^*, \boldsymbol{\psi})]}{\mathbb{E}_{\boldsymbol{\psi} \sim P_{\Psi|\boldsymbol{\theta}^*}^{\star}} [p(\mathbf{y}|\mathbf{x}, \boldsymbol{\theta}^*, \boldsymbol{\psi})]} q(\mathbf{y}|\mathbf{x}, \boldsymbol{\theta}^*) d\mathbf{y} \\ &= \int_{\mathcal{Y}} \log \frac{\mathbb{E}_{\boldsymbol{\psi} \sim Q_{\Psi|\boldsymbol{\theta}^*}} [p(\mathbf{y}|\mathbf{x}, \boldsymbol{\theta}^*, \boldsymbol{\psi})]}{\alpha \mathbb{E}_{\boldsymbol{\psi} \sim Q_{\Psi|\boldsymbol{\theta}^*}} [p(\mathbf{y}|\mathbf{x}, \boldsymbol{\theta}^*, \boldsymbol{\psi})] + (1 - \alpha) \mathbb{E}_{\boldsymbol{\psi} \sim P_{\Psi|\boldsymbol{\theta}^*}^{\star}} [p(\mathbf{y}|\mathbf{x}, \boldsymbol{\theta}^*, \boldsymbol{\psi})]} q(\mathbf{y}|\mathbf{x}, \boldsymbol{\theta}^*) d\mathbf{y} \\ &= - \int_{\mathcal{Y}} \log \left(\alpha + (1 - \alpha) \frac{\mathbb{E}_{\boldsymbol{\psi} \sim P_{\Psi|\boldsymbol{\theta}^*}^{\star}} [p(\mathbf{y}|\mathbf{x}, \boldsymbol{\theta}^*, \boldsymbol{\psi})]}{\mathbb{E}_{\boldsymbol{\psi} \sim Q_{\Psi|\boldsymbol{\theta}^*}} [p(\mathbf{y}|\mathbf{x}, \boldsymbol{\theta}^*, \boldsymbol{\psi})]} \right) q(\mathbf{y}|\mathbf{x}, \boldsymbol{\theta}^*) d\mathbf{y} \\ &= - \int_{\mathcal{Y}} \log \left(\alpha + (1 - \alpha) \frac{p(\mathbf{y}|\mathbf{x}, \boldsymbol{\theta}^*)}{q(\mathbf{y}|\mathbf{x}, \boldsymbol{\theta}^*)} \right) q(\mathbf{y}|\mathbf{x}, \boldsymbol{\theta}^*) d\mathbf{y} \\ &\geq - \log \left(\int_{\mathcal{Y}} \left(\alpha + (1 - \alpha) \frac{p(\mathbf{y}|\mathbf{x}, \boldsymbol{\theta}^*)}{q(\mathbf{y}|\mathbf{x}, \boldsymbol{\theta}^*)} \right) q(\mathbf{y}|\mathbf{x}, \boldsymbol{\theta}^*) d\mathbf{y} \right) \quad (\text{Jensen's inequality}) \\ &= - \log \left(\alpha + (1 - \alpha) \left(\int_{\mathcal{Y}} \frac{p(\mathbf{y}|\mathbf{x}, \boldsymbol{\theta}^*)}{q(\mathbf{y}|\mathbf{x}, \boldsymbol{\theta}^*)} q(\mathbf{y}|\mathbf{x}, \boldsymbol{\theta}^*) d\mathbf{y} \right) \right) \quad (17) \end{aligned}$$

By Definition 3.4, we can say the following about threatening settings:

$$\begin{aligned}
& \mathcal{M}_L^*(\mathbf{x}) > \mathcal{M}_{\text{pred}}(\mathbf{x}) \\
& -\mathcal{M}_L^*(\mathbf{x}) < -\mathcal{M}_{\text{pred}}(\mathbf{x}) \\
& - \int_{\mathcal{Y}} \log \frac{q(\mathbf{y}|\mathbf{x}, \boldsymbol{\theta}^*)}{p(\mathbf{y}|\mathbf{x}, \boldsymbol{\theta}^*)} q(\mathbf{y}|\mathbf{x}, \boldsymbol{\theta}^*) d\mathbf{y} < -\mathcal{M}_{\text{pred}}(\mathbf{x}) \\
& - \log \int_{\mathcal{Y}} \frac{q(\mathbf{y}|\mathbf{x}, \boldsymbol{\theta}^*)}{p(\mathbf{y}|\mathbf{x}, \boldsymbol{\theta}^*)} q(\mathbf{y}|\mathbf{x}, \boldsymbol{\theta}^*) d\mathbf{y} < -\mathcal{M}_{\text{pred}}(\mathbf{x}) \quad (\text{Jensen's inequality}) \\
& \log \int_{\mathcal{Y}} \frac{p(\mathbf{y}|\mathbf{x}, \boldsymbol{\theta}^*)}{q(\mathbf{y}|\mathbf{x}, \boldsymbol{\theta}^*)} q(\mathbf{y}|\mathbf{x}, \boldsymbol{\theta}^*) d\mathbf{y} < -\mathcal{M}_{\text{pred}}(\mathbf{x}) \\
& \int_{\mathcal{Y}} \frac{p(\mathbf{y}|\mathbf{x}, \boldsymbol{\theta}^*)}{q(\mathbf{y}|\mathbf{x}, \boldsymbol{\theta}^*)} q(\mathbf{y}|\mathbf{x}, \boldsymbol{\theta}^*) d\mathbf{y} < e^{-\mathcal{M}_{\text{pred}}(\mathbf{x})} \\
& \quad < 1
\end{aligned} \tag{18}$$

The last line follows since $e^{-\mathcal{M}_{\text{pred}}(\mathbf{x})} \geq 1$ would violate the non-negativity of the Kullback-Leibler divergence measure that defines $\mathcal{M}_{\text{pred}}(\mathbf{x})$.

Since $\int_{\mathcal{Y}} \frac{p(\mathbf{y}|\mathbf{x}, \boldsymbol{\theta}^*)}{q(\mathbf{y}|\mathbf{x}, \boldsymbol{\theta}^*)} q(\mathbf{y}|\mathbf{x}, \boldsymbol{\theta}^*) d\mathbf{y} < 1$, we can say that in the presence of the threat of negative transfer, the expression in line 17 generally decreases with α . Comparison between $\alpha = 0$ and $0 < \alpha \leq 1$ recovers the statement in the theorem. \square

B THE TRADE-OFF BETWEEN ETIG AND ETSIG: A TOY EXAMPLE

Define $\mathbf{x}_{\text{ETIG}} := \text{argmax}_{\mathbf{x}} \text{ETIG}(\mathbf{x})$. We here construct an example in which $\text{ETSIG}(\mathbf{x}_{\text{ETIG}}) = 0$, i.e., in which the action that would be selected by naïve sOED achieves no task identification and thus cannot mitigate $\mathcal{M}_L^*(\mathbf{x})$.

Consider the model $\mathbf{y} \sim \mathcal{N}(\boldsymbol{\theta}x_1 + \boldsymbol{\psi}x_2, \sigma^2)$. The learner's prior over $(\boldsymbol{\Theta}, \boldsymbol{\Psi})$ is $\mathcal{N}(M, S)$ for covariance matrix S with structure $\begin{bmatrix} S_{\boldsymbol{\Theta}} & S_{\boldsymbol{\Theta}, \boldsymbol{\Psi}} \\ S_{\boldsymbol{\Theta}, \boldsymbol{\Psi}}^T & S_{\boldsymbol{\Psi}} \end{bmatrix}$.

$S_{\boldsymbol{\Psi}|\boldsymbol{\theta}} = S_{\boldsymbol{\Psi}} - S_{\boldsymbol{\Theta}, \boldsymbol{\Psi}} S_{\boldsymbol{\Theta}}^{-1} S_{\boldsymbol{\Theta}, \boldsymbol{\Psi}}$ is the variance of $\boldsymbol{\Psi}$ after conditioning on $\boldsymbol{\Theta} = \boldsymbol{\theta}$. The ETIG (Equation (3)) and ETSIG (Definition 3.10) can be calculated analytically as:

$$\text{ETIG}(\mathbf{x}) = \frac{1}{2} \log \left(\frac{\sigma^2 + \mathbf{x}S\mathbf{x}^T}{\sigma^2 + \mathbf{x}S_{\boldsymbol{\Psi}|\boldsymbol{\theta}}\mathbf{x}^T} \right) \tag{19}$$

$$\text{ETSIG}(\mathbf{x}_{\text{ETIG}}) = \frac{1}{2} \left(\log \left(\frac{\sigma^2 + \mathbf{x}S\mathbf{x}^T}{\sigma^2} \right) - \log \left(\frac{\sigma^2 + \mathbf{x}S\mathbf{x}^T}{\sigma^2 + \mathbf{x}S_{\boldsymbol{\Psi}|\boldsymbol{\theta}}\mathbf{x}^T} \right) \right) \tag{20}$$

In this example, $M = [0 \ 0]$, $S_{\boldsymbol{\Theta}} = \sigma_{\boldsymbol{\theta}}^2$, $S_{\boldsymbol{\Theta}, \boldsymbol{\Psi}} = 0$ and $S_{\boldsymbol{\Psi}} = \sigma_{\boldsymbol{\psi}}^2$. The learner can take possible actions of the form

$$\begin{bmatrix} 0 & 0 \\ 1 & 0 \\ \vdots & 0 \\ \overline{x_1} & 0 \\ 0 & 1 \\ 0 & \vdots \\ 0 & \overline{x_2} \end{bmatrix}$$

where $\overline{x_1}$ and $\overline{x_2}$ indicate some upper bound on the values of x_1 and x_2 , respectively. In other words, candidate actions consist of all integer-valued combinations of the variables between 0 and their respective upper bounds, subject to the constraint that at least one of the variables must always be set to 0.

The ETIG for any \mathbf{x} is:

$$\begin{aligned} \text{ETIG}(\mathbf{x}) &= \frac{1}{2} \log \left(\frac{\sigma^2 + \mathbf{x}S\mathbf{x}^T}{\sigma^2 + \mathbf{x}S_{\Psi|\theta}\mathbf{x}^T} \right) \\ \underset{\mathbf{x}}{\text{argmax}} \text{ETIG}(\mathbf{x}) &= \underset{\mathbf{x}}{\text{argmax}} \left(\frac{x_1^2 \sigma_{\theta}^2}{\sigma^2 + x_2^2 \sigma_{\psi}^2} \right) \end{aligned} \quad (21)$$

Equation (19) increases with x_1^2 and decreases with x_2^2 , and so $\mathbf{x}_{\text{ETIG}} = [\bar{x}_1, 0]$. The ETSIG is:

$$\begin{aligned} \text{ETSIG}(\mathbf{x}_{\text{ETIG}}) &= \frac{1}{2} \left(\log \left(\frac{\sigma^2 + \mathbf{x}S\mathbf{x}^T}{\sigma^2} \right) - \log \left(\frac{\sigma^2 + \mathbf{x}S_{\Psi|\theta}\mathbf{x}^T}{\sigma^2} \right) \right) \\ &= \frac{1}{2} (\log(\sigma^2 + \mathbf{x}S_{\Psi|\theta}\mathbf{x}^T) - \log(\sigma^2)) \\ &= \frac{1}{2} (\log(\sigma^2 + x_2^2 \sigma_{\psi}^2) - \log(\sigma^2)) \\ &= \frac{1}{2} (\log(\sigma^2 + 0 \times \sigma_{\psi}^2) - \log(\sigma^2)) \\ &= 0 \end{aligned} \quad (22)$$

C EXPERIMENTAL DETAILS

C.1 Path analysis

To generate the set of possible actions, we sampled 100 values $\mathbf{z} \sim \mathcal{N}(10, .25)$. For each value \mathbf{z} , we then sampled one value of each $\mathbf{x}_{(2)}$, $\mathbf{x}_{(3)}$ and $\mathbf{x}_{(4)}$ from $\mathcal{N}(\mathbf{z}, .25)$, and one value $\mathbf{x}_{(1)}$ from $\mathcal{N}(-1/\mathbf{z}, .25)$. These samples $\{\mathbf{x}_{(1)}, \mathbf{x}_{(2)}, \mathbf{x}_{(3)}, \mathbf{x}_{(4)}\}$ then constituted a set of 100 possible actions the learner could choose among on each time step, where each action set was generated by a unique value \mathbf{z} . The same set of 100 actions was shared in each run of the experiment.

Data was generated according to the model $\mathbf{y} \sim \mathcal{N}(\boldsymbol{\theta}\mathbf{x}_{(1)} + \boldsymbol{\psi}_1\mathbf{x}_{(2)} + \boldsymbol{\psi}_2\mathbf{x}_{(3)} + \boldsymbol{\psi}_3\mathbf{x}_{(4)}, \sigma^2)$ where $\sigma^2 = 1$.

The learner's prior over $(\boldsymbol{\Theta}, \boldsymbol{\Psi}_1, \boldsymbol{\Psi}_2, \boldsymbol{\Psi}_3)$ is $\mathcal{N}(M, S)$ where $M = [0 \ 0 \ 0 \ 0]$ and $S = \begin{bmatrix} 10 & 0 & 0 & 0 \\ 0 & 10 & 0 & 0 \\ 0 & 0 & 10 & 0 \\ 0 & 0 & 0 & 10 \end{bmatrix}$.

We used the formulas given in Equation (19) and Equation (20) to calculate the ETIG and ETSIG, respectively.

To select the generating parameter values for the experiments shown in Figure 3a, we sampled 20,000 parameter values $(\boldsymbol{\theta}, \boldsymbol{\psi}_1, \boldsymbol{\psi}_2, \boldsymbol{\psi}_3)$ from the learner's prior and selected from among these the value with the highest $r^T(\mathbf{x}_{\text{ETIG}}, \boldsymbol{\theta}, \boldsymbol{\psi}_1, \boldsymbol{\psi}_2, \boldsymbol{\psi}_3)$. This is $(-7.46, -5.79, -2.87, -9.36)$.

To select the generating parameter values for the experiments shown in Figure 3c, we selected from among these the value for which $\mathcal{M}_L(\mathbf{x}, \boldsymbol{\theta})$ was closest to $\mathbb{E}_{\boldsymbol{\theta} \sim P_{\boldsymbol{\Theta}}} [\mathcal{M}_L(\mathbf{x}, \boldsymbol{\theta})]$ and $r^T(\mathbf{x}_{\text{ETIG}}, \boldsymbol{\theta}, \boldsymbol{\psi}_1, \boldsymbol{\psi}_2, \boldsymbol{\psi}_3) < 0$. This is $(-3.20, 1.58, 1.75, -2.87)$.

To select the generating parameter values for the experiments shown in Figure 3e, we selected from among these the value with the lowest $r^T(\mathbf{x}_{\text{ETIG}}, \boldsymbol{\theta}, \boldsymbol{\psi}_1, \boldsymbol{\psi}_2, \boldsymbol{\psi}_3)$. This is $(9.33, -3.39, -4.11, -5.17)$.

C.2 Preference modeling

We modified the preference example from [Foster et al. \(2019\)](#), who use a censored sigmoid normal as the output distribution. Instead, we used the Bernoulli distribution $\mathbf{y} \sim \text{Bernoulli} \left(\frac{1}{1 + e^{\boldsymbol{\psi}\mathbf{x} - \boldsymbol{\theta}}} \right)$. In addition, we slightly modify the design space: while in the example in [Foster et al. \(2019\)](#), the learner had possible actions evenly spaced between -80 and 80, our learner had possible actions evenly spaced between -79 and 81. This was to avoid ties, where two different actions could yield the maximum ETIG and be considered \mathbf{x}_{ETIG} , but one elicited negative transfer while the other didn't. In our example, the learner's prior over $(\boldsymbol{\Theta}, \boldsymbol{\Psi})$ was $\mathcal{N} \left([0 \ 0], \begin{bmatrix} 16 & 0 \\ 0 & 1 \end{bmatrix} \right)$.

To select the generating parameter values for the experiments shown in Figure 3b, we sampled 10,000 parameter values $(\boldsymbol{\theta}, \boldsymbol{\psi})$ from the learner's prior and selected from among these the value with the highest $r^T(\mathbf{x}_{\text{ETIG}}, \boldsymbol{\theta}, \boldsymbol{\psi})$. This is $(-16.43, -.32)$.

To select the generating parameter values for the experiments shown in Figure 3d, we selected from among these the value for which $\mathcal{M}_L(\mathbf{x}, \boldsymbol{\theta})$ was closest to $\mathbb{E}_{\boldsymbol{\theta} \sim P_{\boldsymbol{\Theta}}} [\mathcal{M}_L^*(\mathbf{x})\boldsymbol{\theta}]$ and $r^T(\mathbf{x}_{\text{ETIG}}, \boldsymbol{\theta}, \boldsymbol{\psi}) < 0$. This is $(2.21, -.91)$.

To select the generating parameter values for the experiments shown in Figure 3f, we selected from among these the value with the lowest $r^T(\mathbf{x}_{\text{ETIG}}, \boldsymbol{\theta}, \boldsymbol{\psi})$. This is $(8.27, -3.18)$.

Estimating ETIG and ETSIG. Unlike in the path analysis example, for which Equation (19) and Equation (20) give closed-form expressions for the ETIG and ETSIG, the ETIG and ETSIG for this example are not known in closed form. We approximate the posterior distribution with the best-fitting member of a family of variational distributions (Foster et al., 2019). A common choice of variational distribution is a multivariate normal, which is theoretically justified as the asymptotic parameter distribution in the limit of infinite data (Paninski, 2005).

We approximate the posterior distribution as a multivariate normal¹, which allows us to leverage analytical formulations for conditional parameter distributions when estimating the likelihood. Of course, the quality of the ETIG and ETSIG estimates depends on the quality of the variational approximation. If the approximation is biased (in our case, if the true distribution is not a multivariate normal), this will lead to biased estimates of the ETIG and ETSIG. We follow previous work and sample from the variational prior, but correct for bias in this approximation using importance weights (Ryan et al., 2015; Foster et al., 2019; Senarathne et al., 2020). Following Ryan et al. (2015), to construct our variational approximation we inflate the covariance of the best-fitting distribution, and then correct for bias using importance weighting.

Using this method, the estimates of the ETIG and ETSIG corresponding to a given action \mathbf{x} are computed as follows:

$$\widehat{\text{ETIG}}(\mathbf{x}) = \sum_{i=1}^N \left(w(\boldsymbol{\theta}_i, \boldsymbol{\psi}_i) \sum_{\mathbf{y} \in \mathcal{Y}} \left(p(\mathbf{y}|\mathbf{x}, \boldsymbol{\theta}_i, \boldsymbol{\psi}_i) \log \frac{\sum_{j=1}^M w(\boldsymbol{\psi}_j|\boldsymbol{\theta}_i) p(\mathbf{y}|\mathbf{x}, \boldsymbol{\theta}_i, \boldsymbol{\psi}_j)}{\sum_{l=1}^N w(\boldsymbol{\theta}_l, \boldsymbol{\psi}_l) p(\mathbf{y}|\mathbf{x}, \boldsymbol{\theta}_l, \boldsymbol{\psi}_l)} \right) \right) \quad (23)$$

$$\widehat{\text{ETSIG}}(\mathbf{x}) = \sum_{i=1}^N \left(w(\boldsymbol{\theta}_i, \boldsymbol{\psi}_i) \sum_{\mathbf{y} \in \mathcal{Y}} \left(p(\mathbf{y}|\mathbf{x}, \boldsymbol{\theta}_i, \boldsymbol{\psi}_i) \log \frac{p(\mathbf{y}|\mathbf{x}, \boldsymbol{\theta}_i, \boldsymbol{\psi}_i)}{\sum_{l=1}^N w(\boldsymbol{\theta}_l, \boldsymbol{\psi}_l) p(\mathbf{y}|\mathbf{x}, \boldsymbol{\theta}_l, \boldsymbol{\psi}_l)} \right) \right) - \widehat{\text{ETIG}}(\mathbf{x}) \quad (24)$$

Samples subscripted by i and by l are drawn from the variational prior $\hat{p}(\boldsymbol{\theta}, \boldsymbol{\psi})$ (in our implementation, these refer to the same reservoir of samples). Samples subscripted by j are drawn from the conditional variational prior $\tilde{p}(\boldsymbol{\psi}|\boldsymbol{\theta}_i)$, which can be found in analytical form by conditioning the multivariate normal on $\boldsymbol{\theta}_i$. Although not shown explicitly in Equation (23) and Equation (24), each set of M inner samples is constrained to include the corresponding sample $(\boldsymbol{\theta}_i, \boldsymbol{\psi}_i)$ to avoid pathological behavior when a value \mathbf{y} has positive probability in only a very small region of $\hat{P}_{\boldsymbol{\Psi}|\boldsymbol{\theta}_i}$ (Foster et al., 2020). We set N to 10,000 and M to 100 (reflecting results from Rainforth et al. (2018) that M is optimally $\propto \sqrt{N}$).

w indicates the relevant importance weighting function. For example, $w(\boldsymbol{\theta}_i, \boldsymbol{\psi}_i)$ is computed as:

$$w(\boldsymbol{\theta}_i, \boldsymbol{\psi}_i) = \frac{p(\boldsymbol{\theta}_i, \boldsymbol{\psi}_i)/\hat{p}(\boldsymbol{\theta}_i, \boldsymbol{\psi}_i)}{Z^N} \quad (25)$$

where Z^N is a normalizing constant that ensures the N importance weights sum to 1.

Our implementation uses code from the Python library pyBAD for Bayesian active learning under models with Bernoulli likelihood functions (Sloman, 2022, Chapter 2).²

¹Previous work has used the Laplace method (e.g., Ryan et al. (2015); Senarathne et al. (2020)) or stochastic gradient descent (Foster et al., 2019) to construct this approximation. Here, we use a moment-matching approximation in favor of the Laplace method since we observed in a similar setup that it leads to higher effective sample sizes.

²<https://github.com/sabjoslo/pyBAD>